S.R. Mattox TERTIARY VOLCANIC ROCKS - AWAPA PLATEAU UGS Miscellaneous Publication 91-5

PETROLOGY, AGE, GEOCHEMISTRY, AND CORRELATION OF THE TERTIARY VOLCANIC ROCKS OF THE AWAPA PLATEAU, GARFIELD, PIUTE, AND WAYNE COUNTIES, UTAH

by

Stephen R. Mattox
Department of Geology
Northern Illinois University

MISCELLANEOUS PUBLICATION 91-5
UTAH GEOLOGICAL SURVEY
a division of
UTAH DEPARTMENT OF NATURAL RESOURCES

MAY 1991

STATE OF UTAH
Norman H. Bangerter, Governor

DEPARTMENT OF NATURAL RESOURCES
Dee C. Hansen, Executive Director

UTAH GEOLOGICAL SURVEY
M. Lee Allison, Director

BOARD

Member	Representing
Kenneth R. Poulson, Chairman	Mineral Industry
Lawrence Reaveley	Civil Engineering
Jo Brandt	Public-at-Large
Samuel C. Quigley	Mineral Industry
Russell C. Babcock, Jr.	Mineral Industry
Vacant	Mineral Industry
Milton E. Wadsworth	Economics-Business/Scientific
Richard J. Mitchell, Director, Division of State Lands	*Ex officio* member

UGS EDITORIAL STAFF

J. Stringfellow	Editor
Patti F. MaGann, Sharon Hamre	Editorial Staff
James W. Parker, Patricia Speranza	Cartographers

UTAH GEOLOGICAL SURVEY

606 Black Hawk Way
Salt Lake City, Utah 84108-1280

THE UTAH GEOLOGICAL SURVEY is organized into three geologic programs with Administration, Editorial, and Computer Resources providing necessary support to the programs. The ECONOMIC GEOLOGY PROGRAM undertakes studies to identify coal, geothermal, uranium, hydrocarbon, and industrial and metallic mineral resources; to initiate detailed studies of the above resources including mining district and field studies; to develop computerized resource data bases; to answer state, federal, and industry requests for information; and to encourage the prudent development of Utah's geologic resources. The APPLIED GEOLOGY PROGRAM responds to requests from local and state governmental entities for engineering geologic investigations; and identifies, documents, and interprets Utah's geologic hazards. The GEOLOGIC MAPPING PROGRAM maps the bedrock and surficial geology of the state at a regional scale by county and at a more detailed scale by quadrangle. Information Geologists answer inquiries from the public and provide information about Utah's geology in a non-technical format.

THE UGS manages a library which is open to the public and contains many reference works on Utah geology and many unpublished documents on aspects of Utah geology by UGS staff and others. The UGS has begun several computer data bases with information on mineral and energy resources, geologic hazards, stratigraphic sections, and bibliographic references. Most files may be viewed by using the UGS Library. The UGS also manages a sample library which contains core, cuttings, and soil samples from mineral and petroleum drill holes and engineering geology investigations. Samples may be viewed at the Sample Library or requested as a loan for outside study.

The UGS publishes the results of its investigations in the form of maps, reports, and compilations of data that are accessible to the public. For information on UGS publications, contact the UGS Sales Office, 606 Black Hawk Way, Salt Lake City, UT 84108-1280, telephone (801) 581-6831.

The Utah Department of Natural Resources receives federal aid and prohibits discrimination on the basis of race, color, sex, age, national origin, or handicap. For information or complaints regarding discrimination, contact Executive Director, Utah Department of Natural Resources, 1636 West North Temple #316, Salt Lake City, UT 84116-3193 or Office of Equal Opportunity, U.S. Department of the Interior, Washington, DC 20240.

PETROLOGY, AGE, GEOCHEMISTRY, AND CORRELATION OF THE TERTIARY VOLCANIC ROCKS OF THE AWAPA PLATEAU, GARFIELD, PIUTE, AND WAYNE COUNTIES, UTAH

by

Stephen R. Mattox
Department of Geology
Northern Illinois University

MISCELLANEOUS PUBLICATION 91-5
UTAH GEOLOGICAL SURVEY
a division of
UTAH DEPARTMENT OF NATURAL RESOURCES

MAY 1991

THE PUBLICATION OF THIS PAPER
IS MADE POSSIBLE WITH MINERAL LEASE FUNDS

A primary mission of the UGS is to provide geologic information of Utah through publications; the formal publication series is reserved for material whose senior author is a UGS staff member. This Mineral Lease publication provides an outlet for non-UGS authors without necessarily going through extensive policy, technical, and editorial review required by the formal series. It also provides a means for non-UGS authors to publish more interpretive work with the knowledge that readers will exercise some degree of caution.

ABSTRACT

Volcanic rocks of the eastern flank of the Marysvale volcanic field are exposed on the Awapa Plateau, one of the easternmost High Plateaus in the Utah Colorado Plateau - Basin and Range transition zone. Initial mapping by Williams and Hackman (1971) showed the plateau to be similar in lithology and stratigraphy to those to the west. Mudflow breccia of the alluvial facies of the volcanic rocks of Langdon Mountain are exposed at the base of the stratigraphic section. The mudflow breccia records the eastward migration of volcanic debris from andesitic stratovolcanoes on the northern Sevier Plateau in late Oligocene to early Miocene time. Lava flows of William and Hackman's basaltic andesite unit overlie and are interlayered with the mudflow breccia. Isotopic ages determined by the potassium-argon method support synchronous volcanic mudflow deposition and lava flow emplacement. Chemical analyses of the basaltic andesite unit show the lava flows to be trachyandesite in composition. Lava flows of similar age and composition were erupted across the High Plateaus. Trachyte lava flows of William and Hackman's latite unit overlie the mudflow breccia and the basaltic andesite and are early Miocene in age. The Osiris Tuff, an ash-flow of regional extent, overlies all of these units and is interlayered with the mudflow breccia on the western margin of the plateau. By middle Miocene time volcanic sediments had accumulated to produce the Sevier River Formation. Effusive volcanic activity resumed by the middle Miocene and peaked in Miocene - Pliocene time. The resulting shield volcanoes, lava flows, cinder cones, and volcanic necks range from basalt to basaltic trachyandesite in composition and have geochemical characteristics distinct from older mafic lavas.

INTRODUCTION

The Marysvale volcanic field of central Utah covers an area of about 6000 square miles (10,000 square kilometers) to a thickness of at least 3000 feet (900 meters). The Awapa Plateau, on the extreme eastern flank of the Marysvale field, is along the eastern margin of the High Plateaus, a transition zone between the structurally complex, fault-dominated geology of the Basin and Range Province and the nearly flat-lying strata of the the Colorado Plateau (figure 1). Grass Valley, a major structural depression, bounds the Awapa Plateau to the west. Volcanic rocks of age and composition similar to those of the Awapa Plateau lie to the north and to the east on Fish Lake Plateau and Thousand Lake Mountain, respectively. Mesozoic clastic rocks of the Aquarius Plateau extend from beneath the southern margin of the Awapa Plateau volcanic pile. Farther to the west, in the main body of the Marysvale volcanic field, rocks of similar lithology, age, and composition are exposed on the Sevier Plateau, Markagunt Plateau, and in the southern Tushar Mountains.

The Awapa Plateau is one of the least studied areas in Utah. Dutton (1880) noted the wide variety of rocks on the Awapa Plateau and their similarity to rocks to the west. Kennedy (1963) described the volcanic stratigraphy and the structure of Piute County, which includes the westernmost margin of the plateau. The easternmost margin of the plateau was mapped by Smith and others (1963) during an investigation of the Capitol Reef area; a variety of volcanic rocks were grouped in a single map unit. The only geologic map of the entire plateau was prepared by Williams and Hackman (1971) at the scale of 1:250,000. They distinguished several rock units and correlated units with those defined by Callaghan (1939). Callaghan (1973), in a report on the mineral resources of Piute County, mapped the westernmost margin

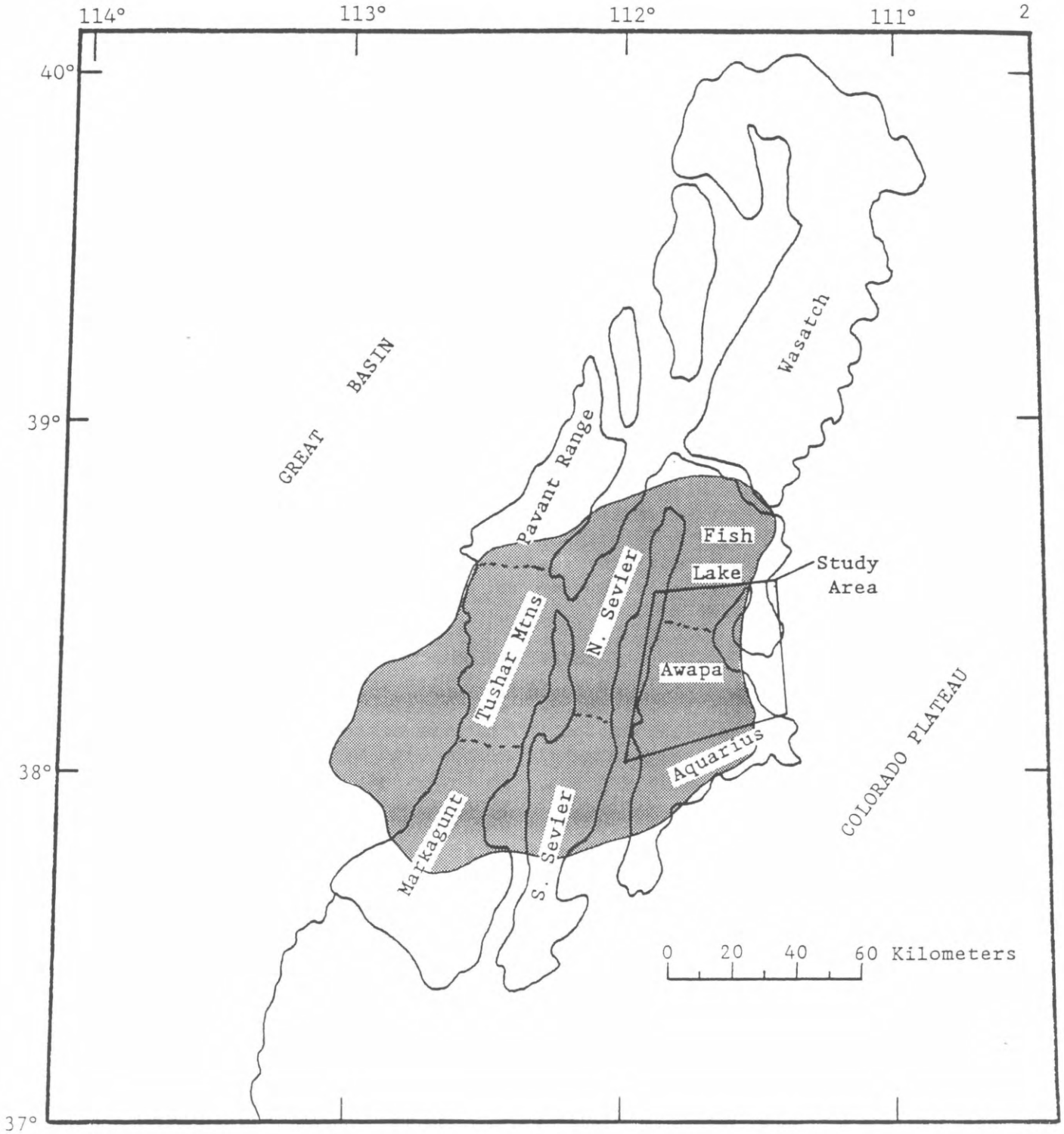

Figure 1. Index map of the High Plateaus of Utah, a sub-province of the Colorado Plateau. Stippled area shows the distribution of volcanic rocks of the Marysvale volcanic field, from Rowley and others (1979).

of the plateau and divided the beds into the units he had defined in 1939. Rowley and others (1986a) mapped the extreme western margin of the Awapa Plateau. They show the Osiris Tuff interlayered with mudflow breccia and the latter overlain by basaltic lava flows.

The primary objectives of this study are: (1) to characterize the petrologic and geochemical variation of the middle and late Cenozoic volcanic rocks of the Awapa Plateau, (2) to constrain the age of the stratigraphic units, (3) to compare the volcanic rocks of the Awapa Plateau to the formally or informally designated stratigraphic units of the High Plateaus to the west, and (4) to outline the middle to late Tertiary geologic history of the Awapa Plateau.

METHODOLOGY

During the summers of 1988 and 1989 nearly 150 samples were collected to represent the stratigraphic and spatial variation of the volcanic rocks of the Awapa Plateau. From these a subset of 12 breccia clasts and 73 lava flows were selected for chemical analysis (Appendix 1, Plate 1). Major elements and phosphorus were determined by multi-element D.C. plasma atomic emission spectroscopy at Northern Illinois University. The procedures detailed in Feigensen and Carr (1985) were used. A mixture of 0.10 gram of sample powder and 1.0 gram of lithium metaborate flux was placed in a graphite crucible. The mixture was melted in a furnace at 1000 degrees celsius for 10 minutes and poured into a Teflon beaker containing 50 milliliters of dilute hydrochloric acid and stirred until dissolved. This solution was used for the analysis of phosphorus. Five milliliters of the original solution was added to 50 milliliters of strontium-doped dilute hydrochloric acid to prepare major-element solutions. Calibration curves were constructed using a variety of U.S.G.S. and French standards. Analytical errors are summarized in Table 1. Trace elements (V, Sc, Ba, La, Cr, Co, Ni, Cu, Zn, Ga, Pb, Th, Rb, Sr, Y, Zr, and Nb) were determined by x-ray fluorescence spectrometry at Northern Illinois University. A mixture of 1.0 gram of sample and 0.5 gram of micro-crystalline cellulose were pressed into disks with a cellulose acetate backing. Mass-absorption effects were corrected by the method of Hower (1959). Geochron laboratories used mineral separates and whole-rock samples for six age determinations by the potassium-argon method. All isotopic ages in this report use or have been converted to the decay constants of the IUGS Subcommission on Geochronology (Dalrymple, 1979; Steiger and Jager, 1977). Thin sections of representative samples from each stratigraphic unit were prepared. No geologic mapping was conducted.

PETROLOGY, COMPOSITION, AGE, AND CORRELATION

Introduction

The rocks exposed on the Awapa Plateau range in age from late Oligocene to late Miocene and total about 3,000 feet (900 meters) in thickness. Mesozoic strata underlie the volcanic sequence and crop out to the east in Capitol Reef and to the south in the Aquarius Plateau. The only stratigraphic division applied to the entire plateau is that of Williams and Hackman (1971), who divided the volcanic sequence into nine units. Field work has shown the utility of Williams and Hackman's divisions and the accuracy of their initial descriptions. Six of their units will be described in greater detail in this report (figure 2). Samples from Williams and Hackman's two undifferentiated units are grouped within the basaltic andesite, latite, or Osiris Tuff, based

TABLE 1
ANALYTICAL ERRORS FOR U.S. GEOLOGICAL SURVEY STANDARD AGV-1

	mean	std. dev.
SiO_2	58.74	0.400
TiO_2	1.03	0.019
Al_2O_3	16.90	0.201
FeO_T	5.99	0.109
MnO	0.095	0.070
MgO	1.48	0.017
CaO	4.84	0.095
Na_2O	3.97	0.757
K_2O	2.79	0.241
V	121.7	3.8
Sc	14.2	1.6
Ba	1141.9	9.7
La	40.8	3.1
Cr	11.2	3.8
Co	16.4	1.1
Ni	18.2	1.0
Cu	61.6	0.8
Zn	89.4	1.4
Pb	36.3	1.2
Th	6.3	1.1
Rb	70.0	0.4
Sr	647.6	2.6
Y	19.9	0.5
Zr	231.2	1.2
Nb	15.9	0.4

Means and standard deviations are based on 10 measurements.
Comparisons are made to the data of Gladney and others (1983).

TABLE 2
K-Ar RADIOMETRIC AGES

Unit	Sample	Latitude(N)	Longitude(W)	Material	K_2O(wt.%)
basaltic andesite	AP47	38° 9'22"	111°49' 5"	plag	3.48
basaltic andesite	AP99	38°23'35"	111°46'42"	plag	3.69
basaltic andesite	AP126	38°14' 3"	111°35'51"	plag	3.29
latite	AP119	38°14'28"	111°38'47"	sanidine	6.48
olivine basalt	AP26	38°45' 5"	111°47'54"	whole rx	1.97
olivine basalt	AP127	38°13'48"	111°35' 8"	whole rx	2.57

Unit	Sample	$^{40}Ar^*$ (10^{-12}mol/g)	$^{40}Ar^*$ (% total)	Calculated date (10^6yr)
basaltic andesite	AP47	28.82	36.0,37.4	25.2±1.6
basaltic andesite	AP99	28.15	50.7,33.7	23.2±1.5
basaltic andesite	AP126	44.32	51.5,40.7	25.8±1.4
latite	AP119	2.49	61.7,81.4,82.6	23.1±1.0
olivine basalt	AP26	33.1	45.8,27.0	16.4±1.0
olivine basalt	AP127	87.2	13.9,13.9	5.9±0.6

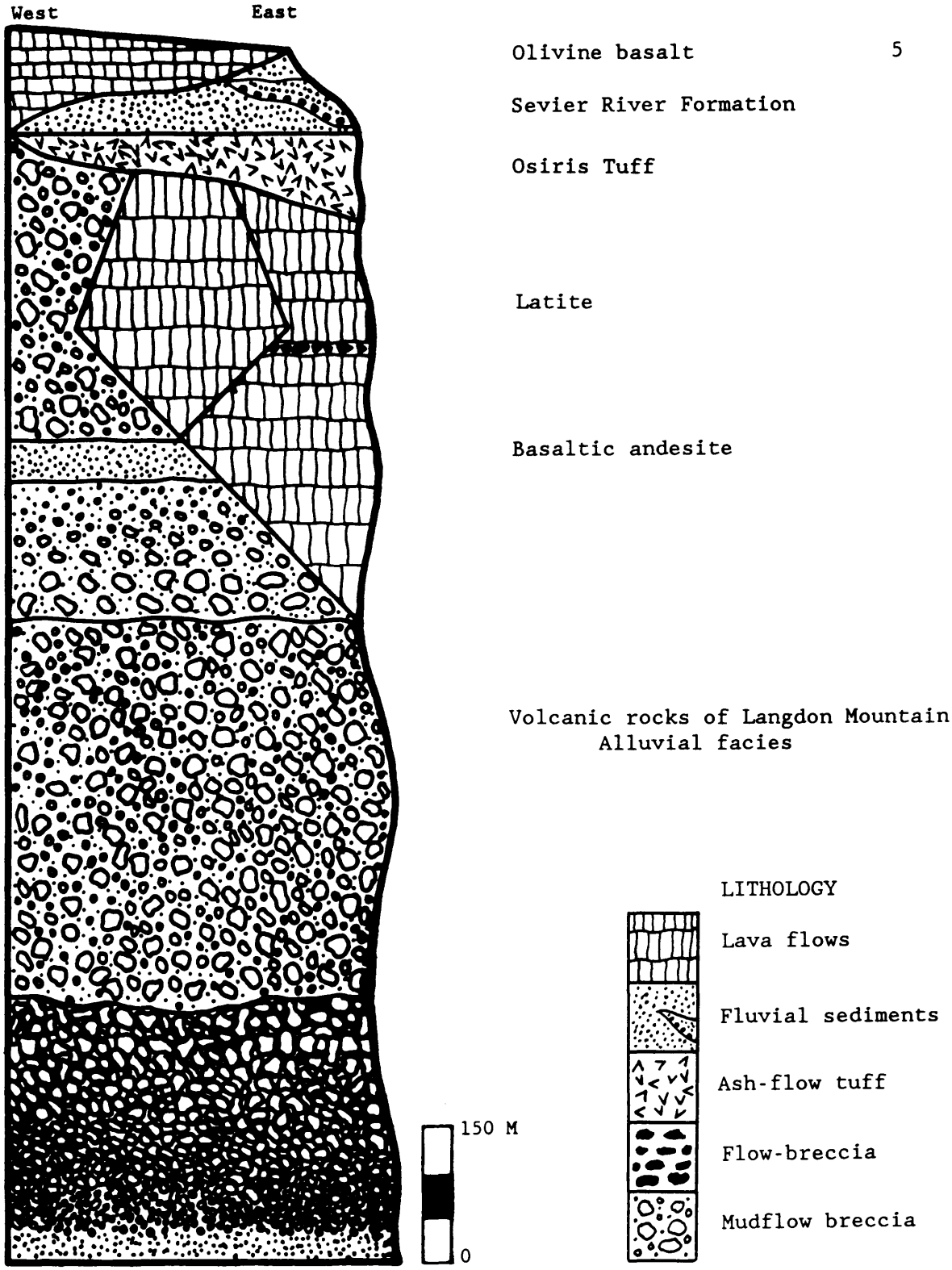

Figure 2. Generalized stratigraphic column for the Awapa Plateau, from Williams and Hackman (1971).

on their mineralogy and chemistry. An undifferentiated sedimentary rock unit (Tsc, Williams and Hackman, 1971) is not described in this study.

The oldest exposed rocks along the base of the western front of the plateau consist of volcanic mudflow breccia, an alluvial facies of the volcanic rocks of Langdon Mountain, an informal stratigraphic unit first described on the Sevier Plateau (Rowley, 1979; Rowley and others, 1986a). The unit was originally termed andesite breccia by Williams and Hackman (1971) (figure 2). The mudflow breccia thins to the east and is covered by lava flows of basaltic andesite that form the base of the exposed section on the east front (Plate 2). Both units are late Oligocene to earliest Miocene. Latite lava flows are interlayered with the upper portion of both units. The Osiris Tuff, with an age of about 23 Ma (Fleck and others, 1975), overlies the basaltic andesite and the latite on the eastern half of the plateau but interfingers with the mudflow breccia in the west (Rowley and others, 1986a). Siltstone, sandstone, and conglomerate of volcanic material, termed volcanic sediments by Williams and Hackman, overlie all of the above mentioned units and are classified as the Sevier River Formation. Lava flows, cinder cones, and volcanic necks of olivine basalt overlie all units. Best and others (1980) established an age range of 6.5 to 5.0 m.y. for the olivine basalt flows along the southwestern margin of the Plateau.

Volcanic rocks of Langdon Mountain

The lowest stratigraphic unit exposed on the Awapa Plateau consists of volcanic mudflow breccia, conglomerate, and sandstone. Williams and Hackman (1971) grouped these rocks in their andesite breccia unit. Later, more detailed studies on the northern Sevier Plateau revealed "a stratovolcano sequence of andesitic to dacitic, massive to well-bedded volcanic mudflow breccia and subordinate flow breccia, lava flows, and fluvial sandstone and conglomerate" (Rowley and others, 1986a) that was informally designated the volcanic rocks of Langdon Mountain (Rowley, 1979; Rowley and others, 1979). Mapping by Rowley and others (1986a) showed the alluvial facies of the volcanic rocks of Langdon Mountain extended to the western margin of the Awapa Plateau. Systematic variation in clast size and bedding characteristics in the volcanic mudflow breccia across the Awapa Plateau support the assignment of this unit to the alluvial facies of the volcanic rocks of Langdon Mountain.

Excellent exposures of the mudflow breccia are produced by the large displacement on the Paunsaugunt fault. The sequence is greater than 2,600 feet (800 m) thick and forms near-vertical cliffs along much of the length of Parker Mountain (Plate 1). The andesite breccia also crops out in the hills at the base of the mountain front. Clast-supported, polymictic, polymodal breccia dominates; the strata weather medium gray to brown. As the matrix content increases the steepness of the outcrop tends to decrease. Light-gray, plagioclase- and hornblende-phyric clasts are by far the most common (samples AP36, 37, 65, and 93)(figure 3). Dark-gray, plagioclase-phyric clasts were also found at most exposures (AP40, 42, and 92). Clasts range in size from pebbles to boulders and reach a maximum long-axis length of 9 feet (2.7 meters). Structureless beds 30 to 50 feet (9 to 15 m) thick have scoured basal contacts; internally they are crudely stratified on a scale of 1 to 10 feet (0.3 to 3 m).

With the exception of a few deeply dissected canyons, exposures on the plateau are poor. At Big Hollow, 9 miles (14.4 kilometers) from the plateau's

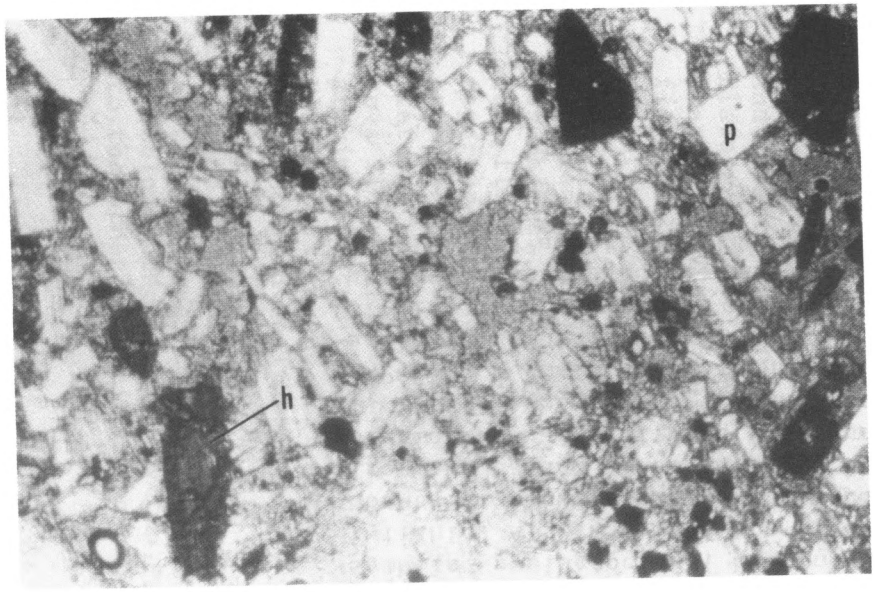
p
h

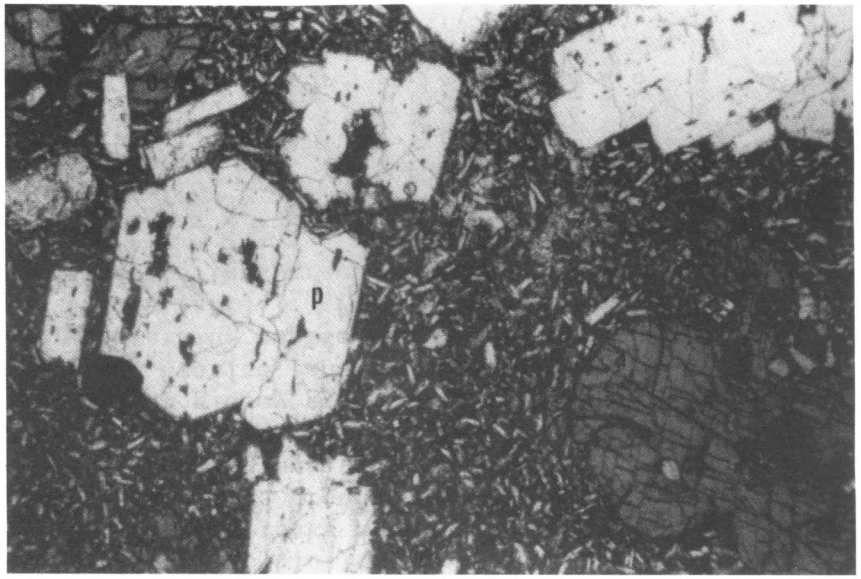
p

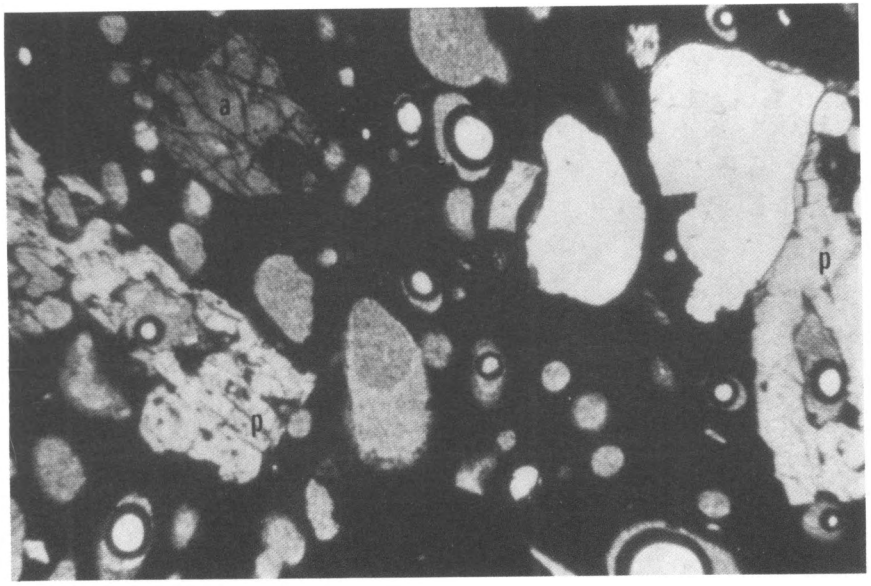
a
p
p

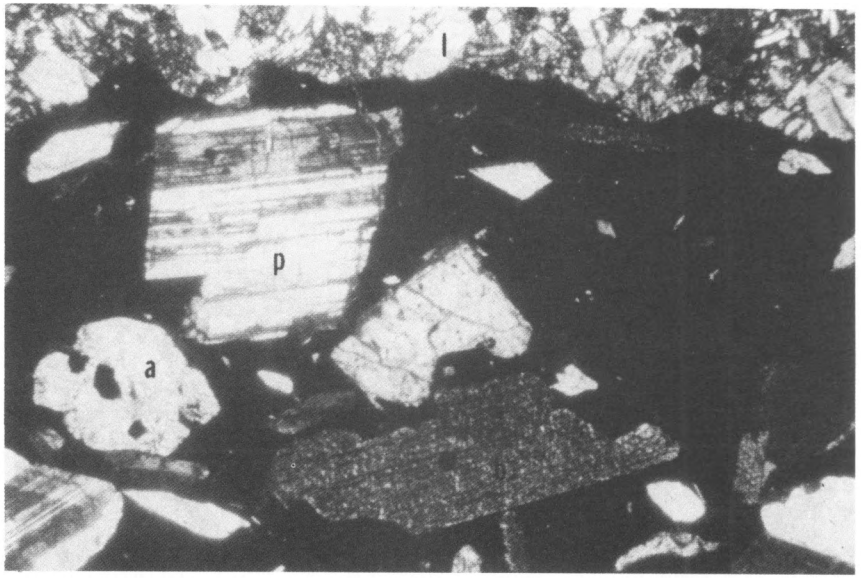
l
p
a

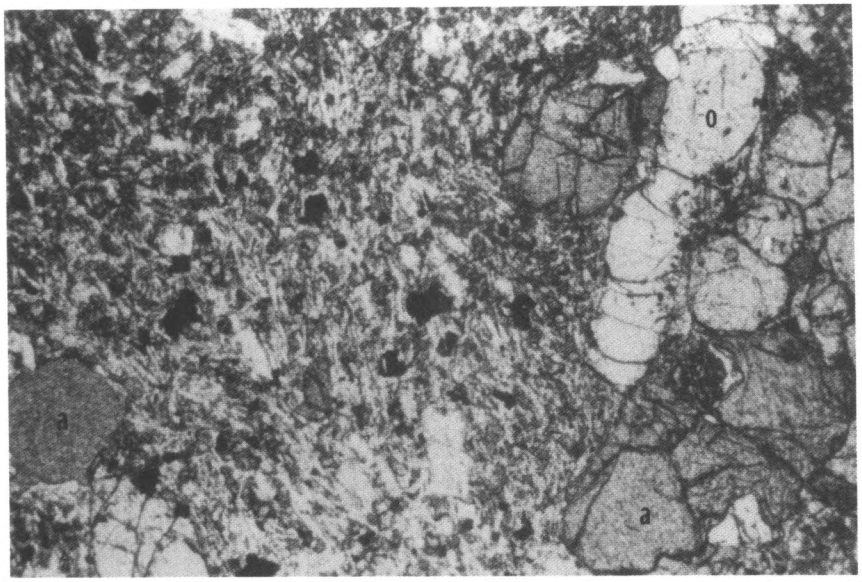

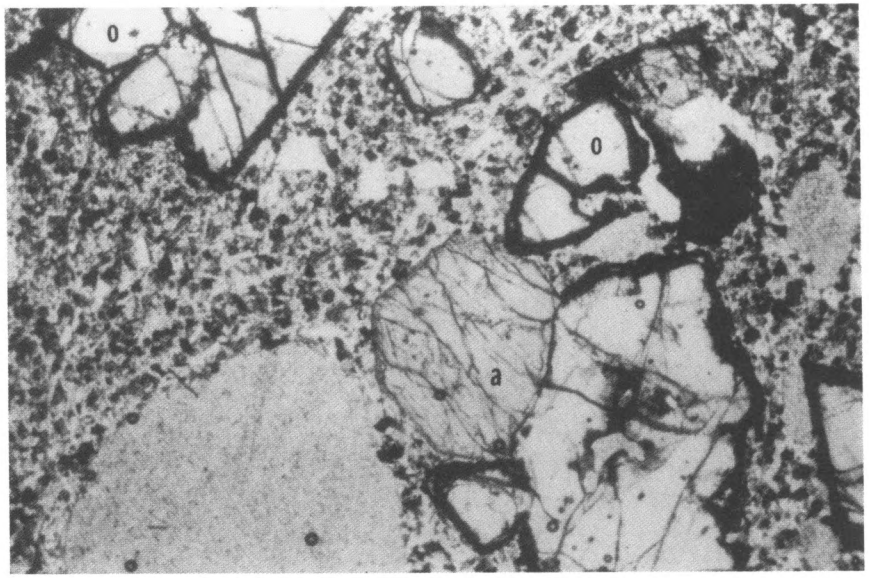

Figure 3. Photomicrographs of representative samples from each stratigraphic unit. All photomicrographs are in plane-polarized light and are 4 mm across. Symbols: p=plagioclase, h=hornblende, a=augite, o=olivine, b=biotite, and l=lithic. A. Clast from the alluvial facies of the volcanic rocks of Langdon Mountain, showing plagioclase and hornblende phenocrysts in a groundmass of iron oxides and glass (AP36). B. Basaltic andesite, showing augite, resorbed plagioclase, and olivine in a groundmass of plagioclase microlites (AP114). C. Latite, showing augite and resorbed plagioclase in a glassy groundmass (AP69). D. Osiris Tuff, showing plagioclase, augite, biotite, and lithics in a glassy groundmass (AP91v). E. Olivine basalt, containing augite and fresh olivine in a groundmass of plagioclase and iron oxides (AP131). F. Olivine basalt, containg augite and olivine rimmed by iddingsite in a groundmass of plagioclase and iron oxides (AP107).

western front, nearly 300 feet (90 meters) of well-stratified volcaniclastic sandstone and conglomerate comprise the uppermost part of the volcanic rocks of Langdon Mountain section. Beds of this sandstone and conglomerate range from 1 to 6 feet (0.3 to 2 meters) thick and range from well-sorted tuffaceous sandstone or clast-supported conglomerate to poorly-sorted, matrix-supported cobble and/or boulder conglomerate in a tuffaceous matrix. Composition of the clasts in the conglomerate is similar to that along the western front except for sample AP72, which appears to be a hornblende cumulate. The maximum long-axis length of a boulder is five feet (1.5 m). Beds are structureless, inversely graded, or normally graded. Palmer and Walton (1990) and Walton and Palmer (1988) described similar facies to the west.

The volcanic rocks of Langdon Mountain on the Awapa Plateau have not been dated. No attempt was made to determine the age of clasts within the breccia by the potassium-argon method because of the known difficulties in interpreting such ages. Two lava flows in the overlying basaltic andesite unit provide ages of about 25 m.y. (see below). On the western margin of the plateau the Osiris Tuff, a 23 m.y. old ash-flow tuff (Fleck and others, 1975), is interlayered with the upper part of the mudflow breccia. Based on these isotopic ages the breccia must range in age from late Oligocene to early Miocene.

Clasts from the andesite breccia range from basaltic andesite to trachyandesite and dacite in composition (figure 4). One clast (AP72), not shown in figure 4 because of its non-representative chemistry, consists entirely of centimeter-sized hornblende phenocrysts and is a basanite in composition.

On nearly all of the High Plateaus the lowermost exposed volcanic-stratigraphic unit is a thick sequence of vent-facies lava flows flanked by alluvial-facies mudflow breccia. In the Tushar Mountains, the Bullion Canyon Volcanics contain at least 3,300 feet (1,000 meters) of lava flows, flow breccia, mudflow breccia, subordinate conglomerate and sandstone, and several interlayered ash-flow tuffs (Rowley and others, 1979). Rhyodacite lava flows are most common and contain phenocrysts of plagioclase, biotite, hornblende, and lesser pyroxene (Cunningham and others, 1983). On the northern Markagunt Plateau and the southern Sevier Plateau, the Mount Dutton Formation, an assemblage of crystal-poor dacitic to andesitic lava flows, flow breccia, and mudflow breccia with local accumulations of felsic volcanic rocks and tuffaceous sandstone (Anderson and others, 1990 a and b), has a maximum thickness of about 2000 feet (600 meters)(Rowley and others, 1987). Blackman (1985), in a detailed examination of Mount Dutton vents near Circleville, found four mafic assemblages: pyroxene-phyric lava flows, transitional pyroxene and hornblende lava flows, and hornblende-phyric lava flows. Similar mineral assemblages are reported elsewhere in the Mount Dutton Formation (Anderson and Rowley, 1987; Anderson, 1986; and Anderson and others, 1987). On the northern Sevier Plateau the volcanic rocks of Langdon Mountain contain andesitic and dacitic lava flows, flow breccia, and fluvial sandstone and conglomerate, with an approximate total thickness of 350 meters (Rowley and others, 1986a). Plagioclase is the most common phenocryst with subordinate hornblende, pyroxene, and Fe-Ti oxides. The basal sequence of the Awapa Plateau is almost entirely mudflow breccia; no lava flows or flow breccia are present. Plagioclase and hornblende, with minor amounts of clinopyroxene, comprise the phenocryst assemblage of the breccia clasts. Based on stratigraphic position, lithology, and mineralogy the mudflow breccia of the Awapa Plateau is similar to the other volcanic rocks exposed to the west in the High Plateaus. More

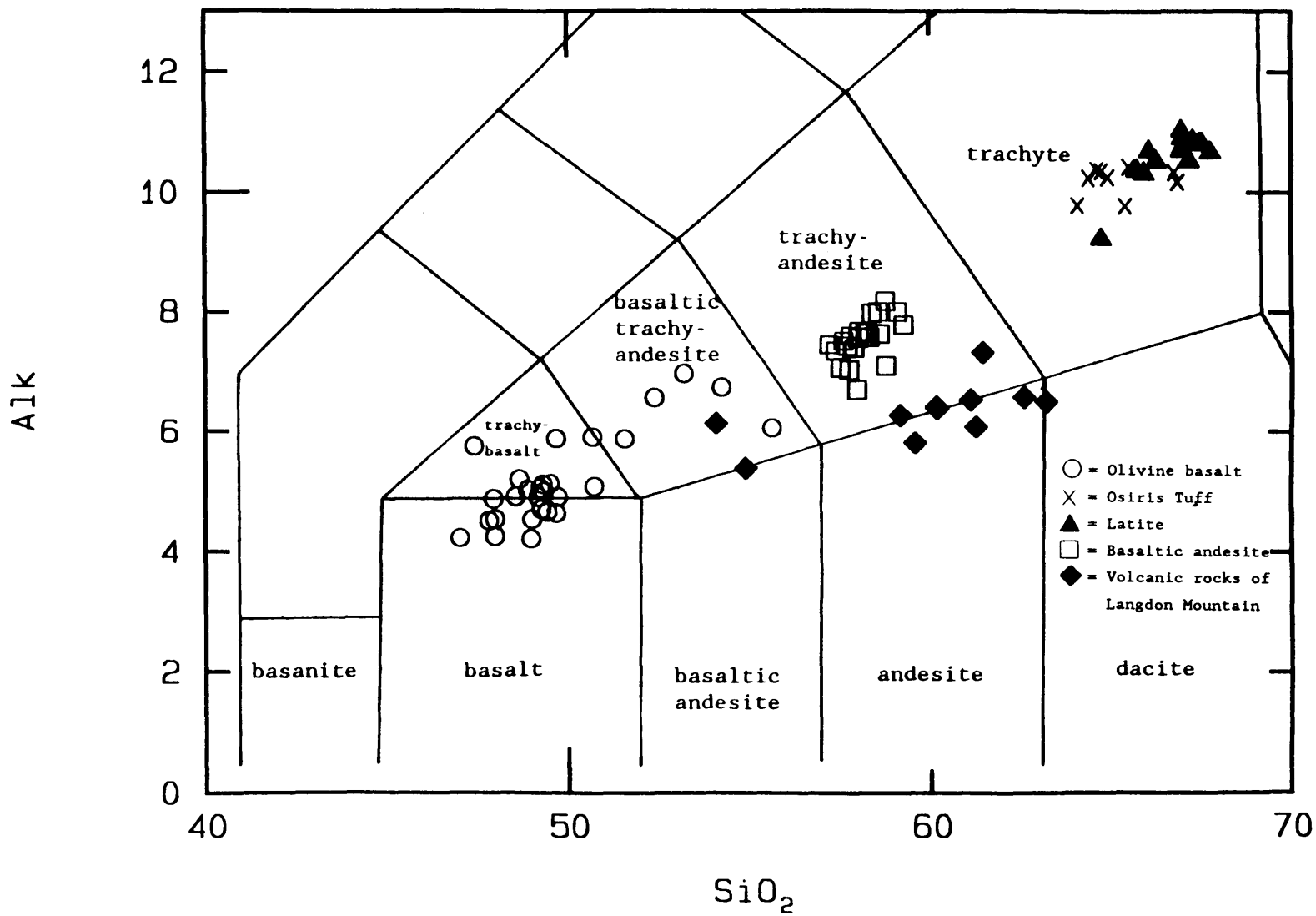

Figure 4. IUGS classification of volcanic rocks (Le Bas and others, 1986) of the Awapa Plateau.

than 92 samples from lava flows of the Mount Dutton Formation (Mattox, unpublished data) define a field in figure 5. Clasts from the mudflow breccia of the Awapa Plateau plot within the field, and attest to the compositional similarity of the two units. Rowley and others (1986a) mapped the mudflow breccia at the base of Parker Mountain as alluvial facies of the volcanic rocks of Langdon Mountain and suggested local sources on the Awapa Plateau. Based on stratigraphic position, lithology, and mineralogy Rowley and others' assignment is correct but the gentle eastward dip of these strata, the lack of lava flows, the eastward decrease in maximum clast size, abundance of breccia, bed thickness, and the lack of similar beds in Thousand Lake Mountain point to a source on the northern Sevier Plateau. The mudflow breccia undoubtedly is the distal alluvial facies of a stratovolcano complex whose vents are in the northern Sevier Plateau, probably the Langdon Mountain area.

Basaltic Andesite

Lava flows and flow breccia of Williams and Hackman (1971)'s basaltic andesite unit overlie the volcanic rocks of Langdon Mountain. The two units are laterally equivalent on the eastern portion of the plateau where lenses of basaltic andesite are surrounded by mudflow breccia. Maximum exposed thickness of basaltic andesite is approximately 300 feet (90 meters) at Black Point and in Long Hollow (S sec. 16, T.28S., R.2E.). Williams and Hackman (1971) reported a maximum thickness of 700 feet (210 meters). The well exposed lava flows capping Boulder Mountain east of the Awapa Plateau allowed Smith and others (1963) to distinguish three flows in a section 475 feet (145 meters) thick. An excellent exposure of a lava flow is provided by a road cut at Black Point. Flow breccia is exposed in a roadcut north of Loa (NENW sec. 36, T.27S., R.2E.)(sample AP87). Elsewhere the unit weathers to discontinuous ledges or boulder-strewn hillsides. Medium-gray to black porphyritic lava flows contain nearly equal amounts of clinopyroxene (0.2 to 3.5 mm, typically 1 to 3 mm) and sieved-textured, embayed plagioclase (0.3 to 1.0 mm)(figure 3). Olivine (0.2 to 1.0 mm, typically 0.2 to 0.5 mm), in part altered to iddingsite, orthopyroxene (0.2 to 2.5 mm), and iron oxides (0.1 to 1.0 mm) are less abundant. The groundmass is dominated by plagioclase microlites and various amounts of iron oxides and glass. Vesicles are common and elongate in the direction of flow.

Using the potassium-argon method, Best and others (1980) dated a sample from Williams and Hackman's latite and basaltic andesite flows undifferentiated, collected north of the Awapa Plateau near the southern end of Fish Lake. An age of 24.5 m.y. was obtained. Samples AP27 and AP28 of this study are from this locality and, based on their mineralogy and chemistry, have been reassigned to the basaltic andesite. Three samples collected in this study have been dated by the potassium-argon method. Sample AP47 was collected east of the Tanks (Plate 1) from lava flows originally mapped as latite by Williams and Hackman (1971). The chemistry of the sample is indistinguishable from that of the basaltic andesite lava flows and is therefore grouped with the basaltic andesite. The sample yielded an age of 25.2±1.6 m.y.. Sample AP99 was collected from the top of the basaltic andesite section, just below the Osiris Tuff, and yielded an age of 23.2±1.5 m.y.. Sample AP26 was collected from the extreme eastern margin of the Awapa Plateau and yielded an age of 25.8±1.4 m.y..

Lavas flows from the basaltic andesite unit are trachyandesite in composition (figure 4). All samples from the Awapa Plateau contain more than

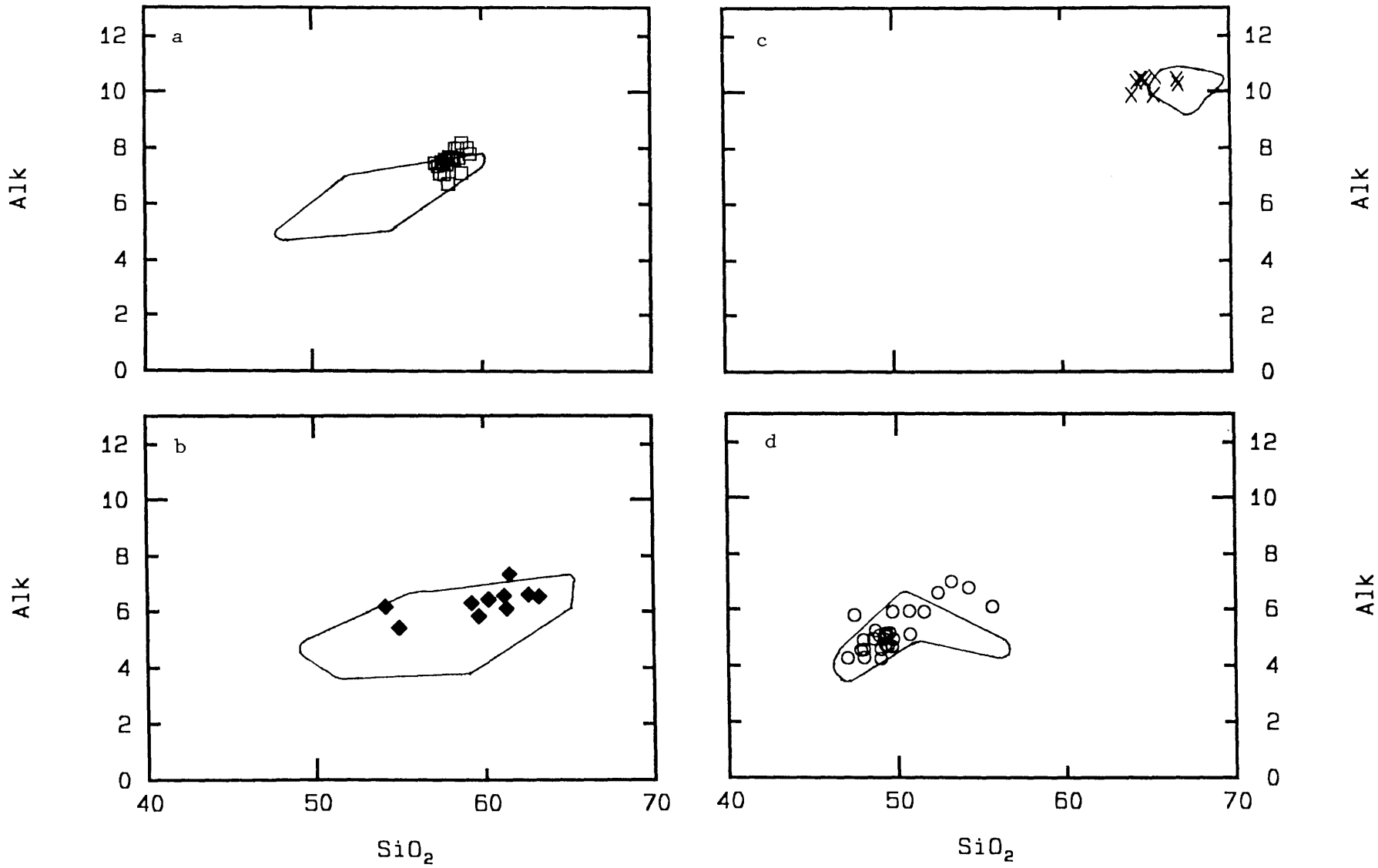

Figure 5. Chemical correlation of total alkalies versus silica for: a. volcanic rocks of Langdon Mountain versus Mount Dutton Formation; b. Basaltic andesite from the Awapa Plateau versus potassium-rich lava flows (Steven and others, 1990); c. Osiris Tuff versus Osiris Tuff from the type locality (10 samples) and other plateaus (5 samples); d. Olivine basalts from the Awapa Plateau versus the basalt lava flows of Steven and others (1990). Fields of rock compositions used for comparison to the Awapa Plateau samples are from Mattox (unpublished data).

3 weight percent K_2O, a characteristic shared with mafic lava flows of similar age to the west (Steven and others, 1990). Trace-element abundances suggest that the unit can be divided. Large-ion lithophile elements (Ba, Sr) are enriched in samples from the northern Awapa Plateau. Samples from Thousand Lake Mountain and south of Bicknell Bottoms have lower concentrations of these elements (figure 6). Five samples (AP21, 24, 27, 28, and 47) from Williams and Hackman's basaltic andesite and latite undifferentiated unit were reassigned to the basaltic andesite unit because of their mineralogy and major- and trace-element chemistry.

Based on stratigraphic position, lithology, mineralogy, texture, chemical composition, and age, the basaltic andesite unit is correlative to the potassium-rich mafic lava flows, volcaniclastic breccia, and conglomerate of Steven and others (1990), potassium-rich mafic volcanic rocks in the Southern Tushar Mountains of Cunningham and others (1983), the mafic lava flows of Birch Creek Mountain of Anderson and others (1990 a and b), the mafic lava flows of Circleville Mountain of Anderson (1986), and to the lava flows of Riley Spring of Nelson (1989). At most locations, laterally continuous sheets of mafic lava of shield or fissure origin lie unconformably above mudflow breccia. On the Sevier Plateau, Anderson and Rowley (1975, p. 34) described olivine- and magnetite-phyric basalt "in a groundmass of glass and crystallites of plagioclase and ferromagnesian minerals." In the southern Tushar Mountains, mafic lava flows contain "small subhedral crystals and large (as much as 1 cm) glomeroporphyritic clusters of augite, with sparse amphibole and olivine (commonly altered to iddingsite)" (Anderson and Rowley, 1975, p. 35) in a glassy groundmass of plagioclase laths and magnetite. All of the above mentioned phenocrysts are observed in the basaltic andesite of the Awapa Plateau but clinopyroxene, not olivine, appears to be the most common. Glomeroporphyric texture of olivine, clinopyroxene, orthopyroxene, and plagioclase was observed in samples AP99 and AP126. The groundmass ranges from glass to plagioclase microlites. Iron oxides are ubiquitous in the groundmass. Unlike the potassium-rich lavas to the west, plagioclase is a common phenocryst in the basaltic andesite of the Awapa Plateau. Nearly 30 samples from potassium-rich mafic volcanic rocks of the Southern Tushar Mountains, mafic lava flows of Birch Creek Mountain, and the mafic lava flows of Circleville Mountain define a field in figure 5 (Mattox, unpublished data). The Awapa Plateau samples fall within a restricted area in this field. The basaltic andesite is remarkably similar in major- and trace-element chemistry to the lava flows of Riley Spring. For example, compare samples 1 and 2 of Nelson (1989, Table 2) to samples AP126 and AP114 (Appendix 2), respectively. Ages for the potassium-rich lava flows to the west range from 23 to 21 m.y. (Fleck and others, 1975; Best and others, 1980). Best and others (1980) also reported an age of 24.5 m.y. for a potassium-rich lava just north of the Awapa Plateau. The lava flows of Riley Spring are 23.8 m.y. old (Nelson, 1989). Isotopic ages for samples from this study range from 25.8 to 23.2 m.y. Apparently potassium-rich volcanism began in the east. The distribution of the ages does not support a westward migration of activity but might reflect early eruptions ringing the Marysvale field. The older ages for the basaltic andesite are supported by their stratigraphic position beneath the Osiris Tuff. Steven and others (1979) described a broad shield volcano centered on the northern Sevier Plateau that may have been the source for the basaltic andesite lava flows of the Awapa Plateau.

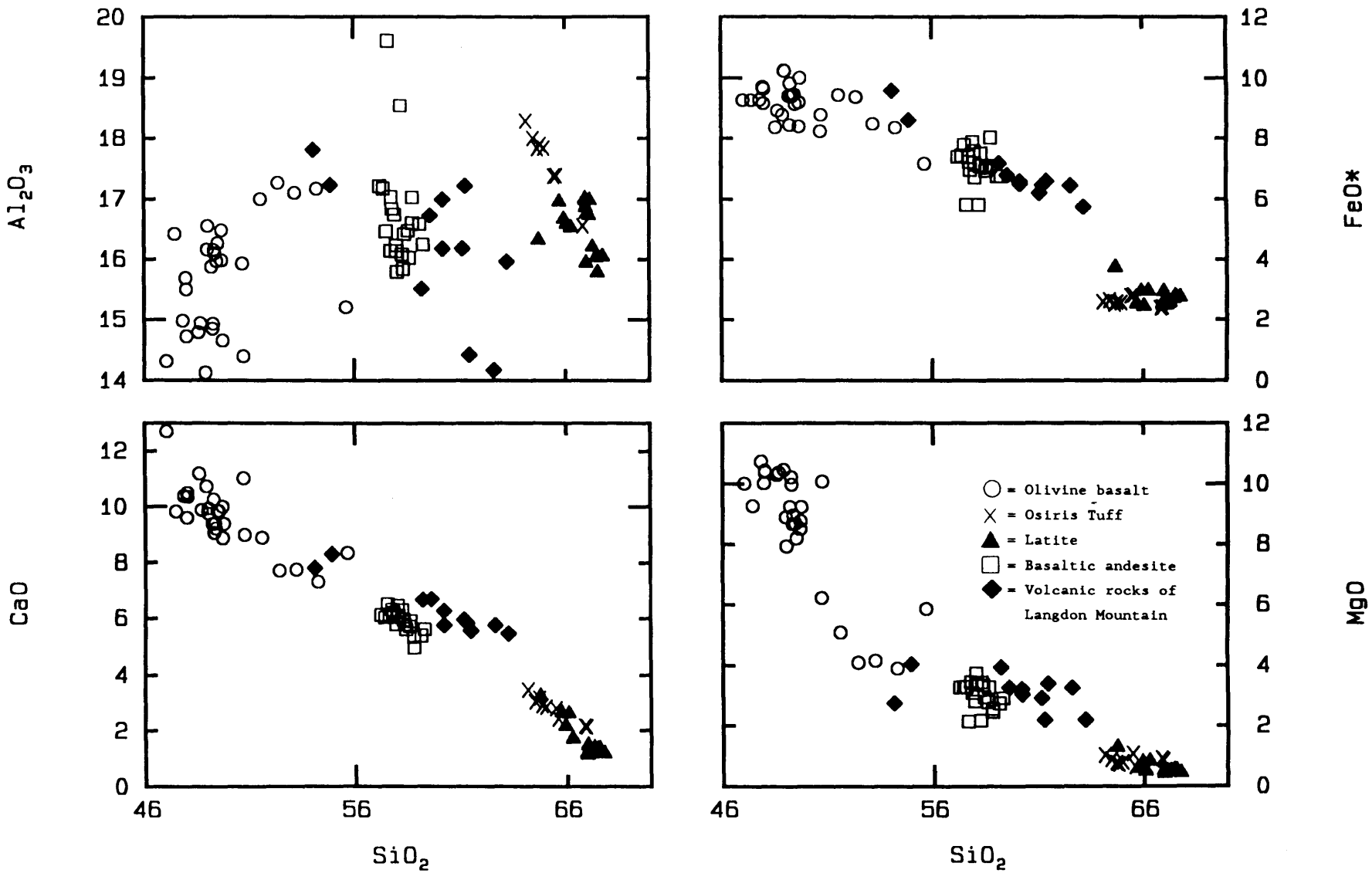

Figure 6. Major- and trace-element variation diagrams for volcanic rocks of the Awapa Plateau.

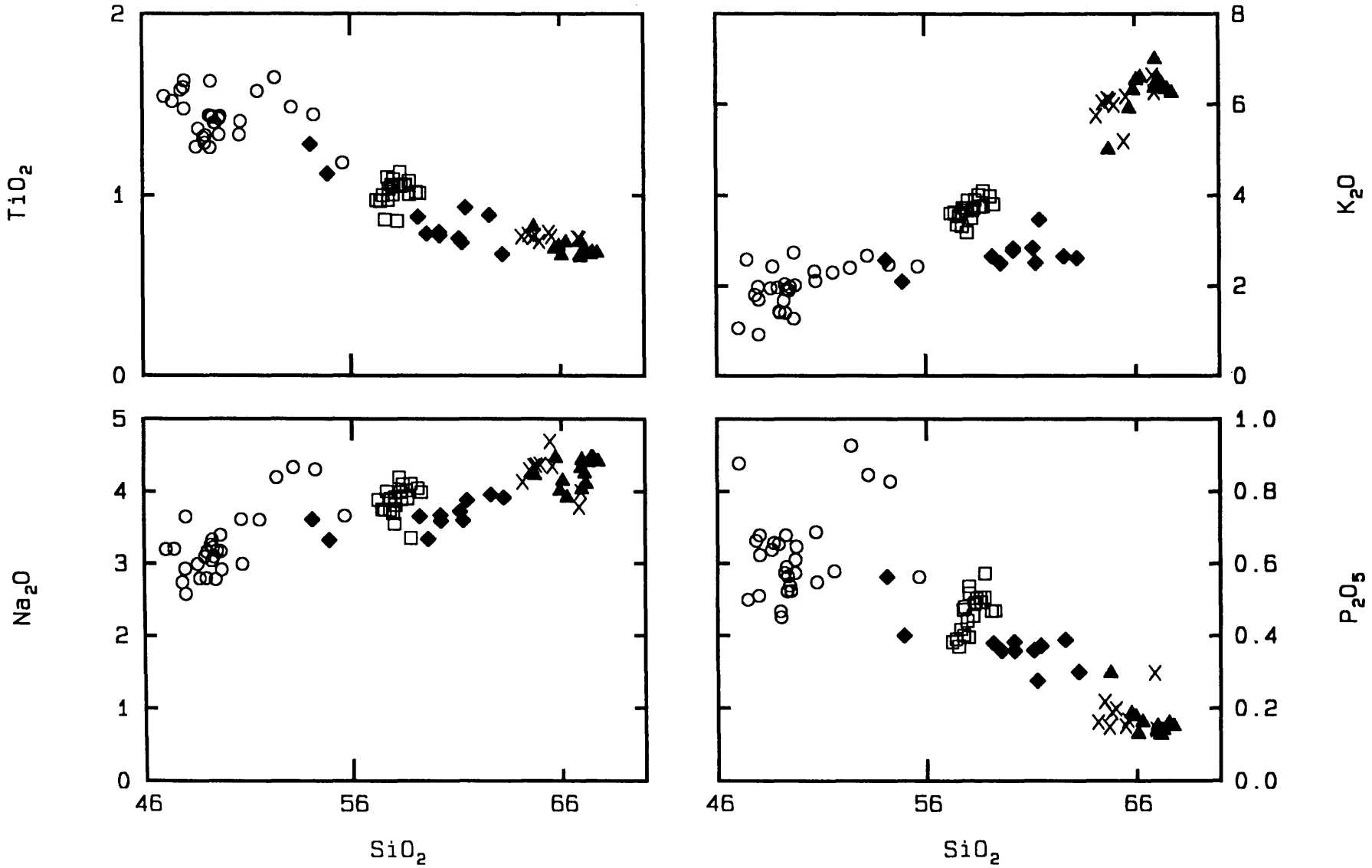

Figure 6 continued.

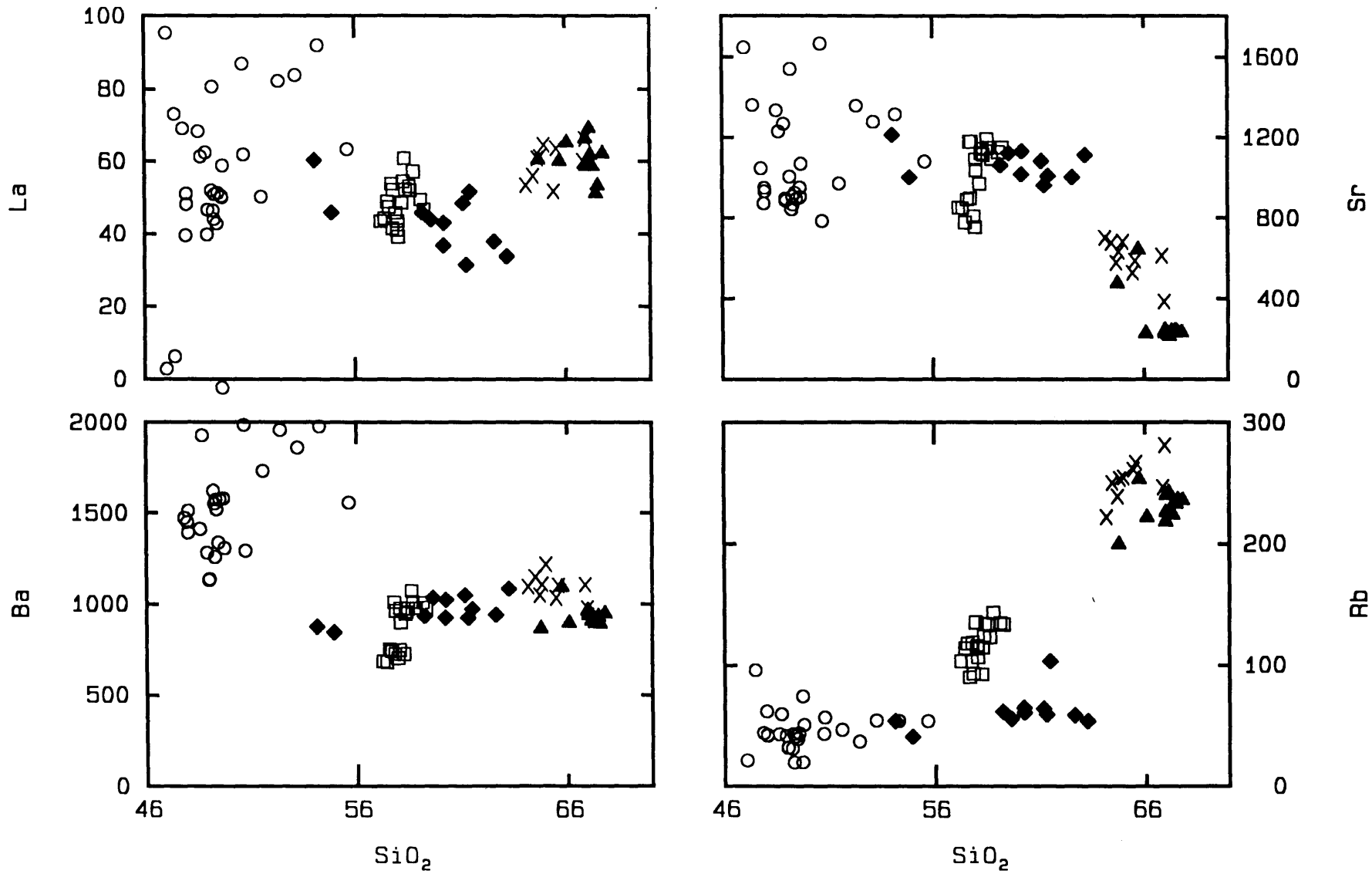

Figure 6 continued.

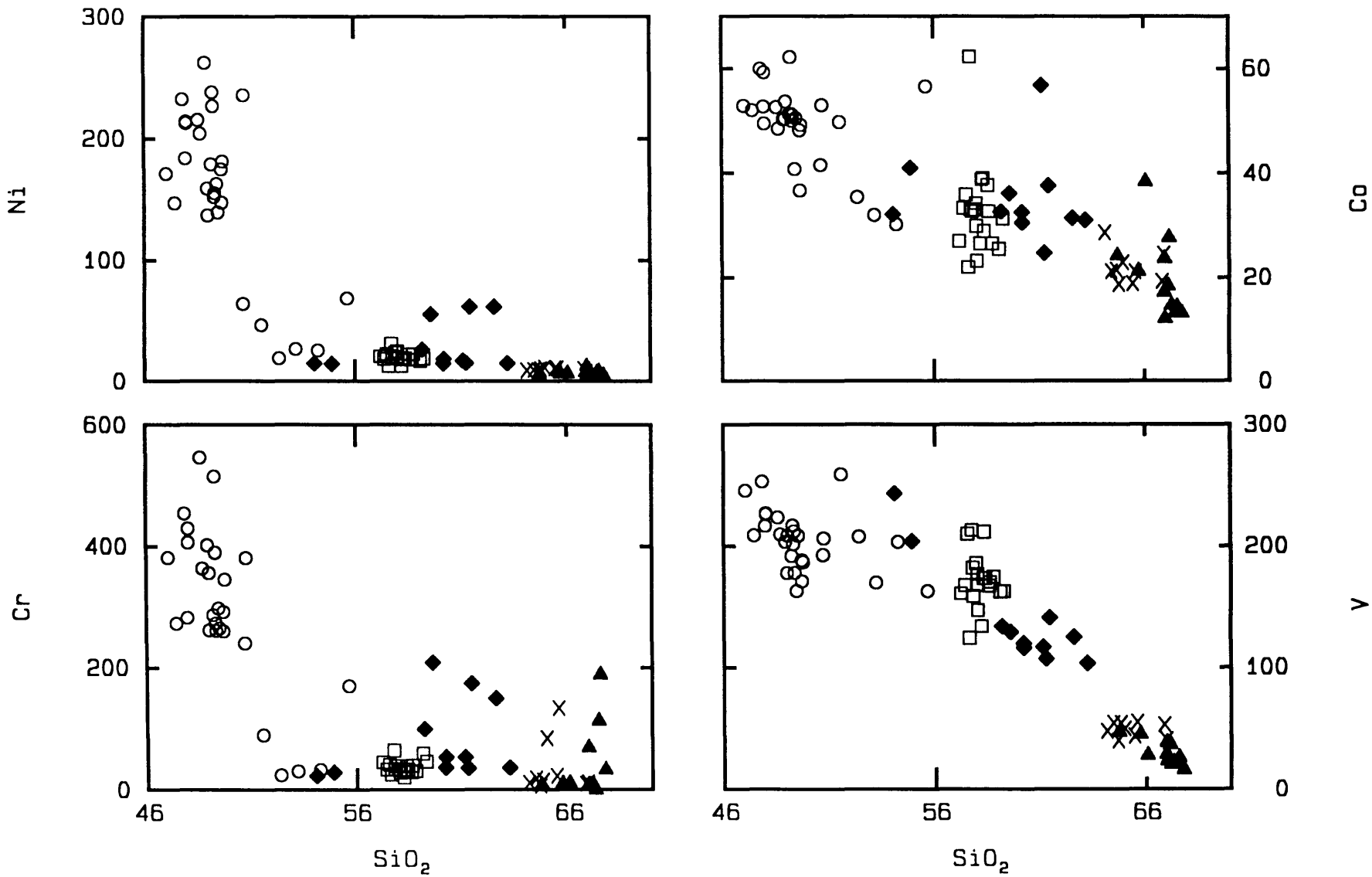

Figure 6 continued.

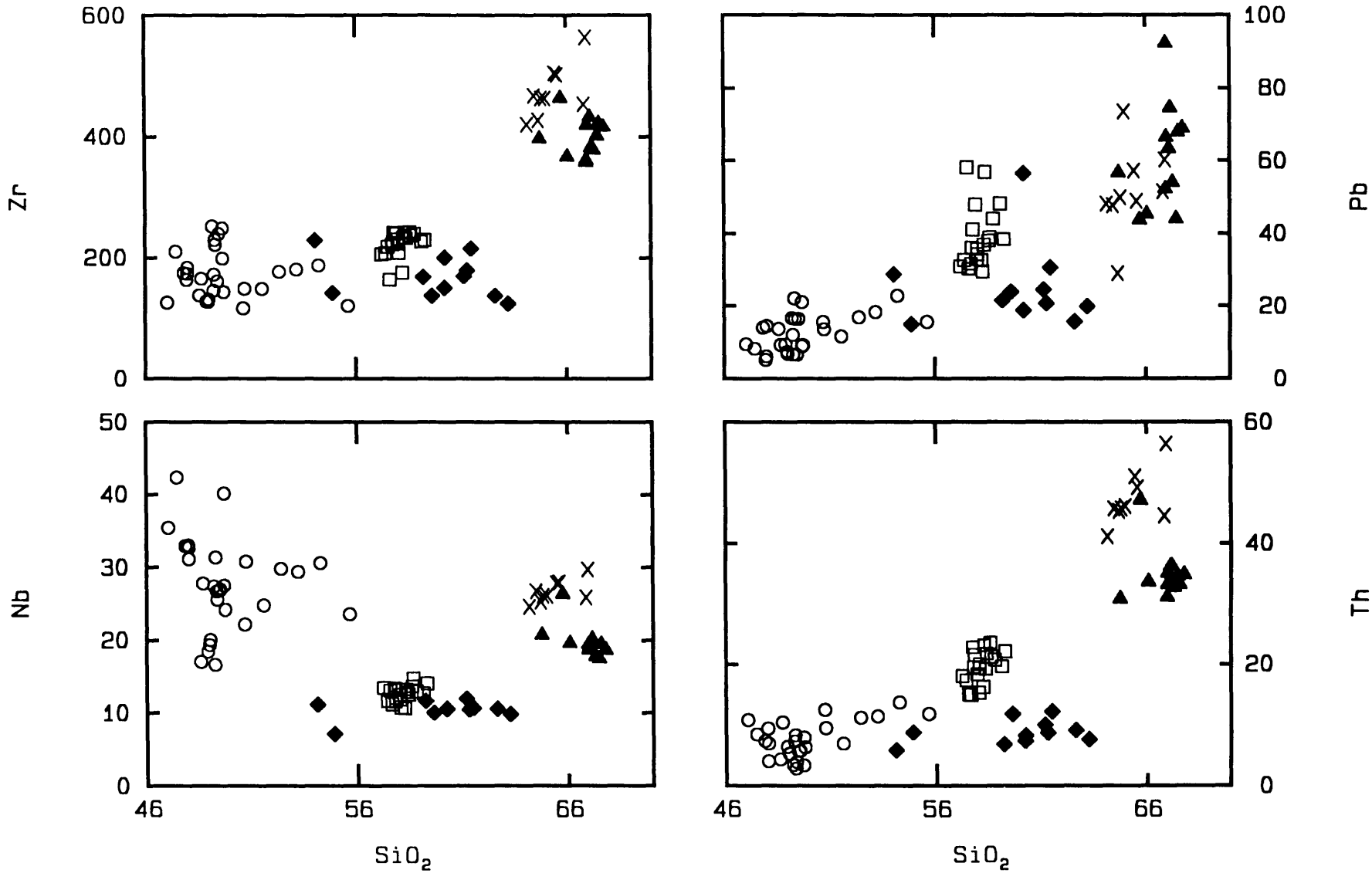

Figure 6 continued.

Latite

Lava flows of the latite unit of Williams and Hackman (1971) are interlayered with the alluvial facies of the volcanic rocks of Langdon Mountain and the basaltic andesite. At most exposures the unit has weathered to large boulders; however, in the lower reaches of Big Hollow (secs. 11, 12, 13, and 14, T.29S., R.2E.), latite lava flows nearly 500 feet thick (150 meters) form cliffs that overlie the mudflow breccia. In upper Wildcat Hollow (NESW sec. 36, T.29S., R.2E.), discontinuous outcrops of platy latite are more than 300 feet (90 meters) thick and can be separated into at least three differerent flows. Southeast of Bicknell Bottoms (NE sec. 15, T.29S., R.3E.) a resistant latite layer rests on basaltic andesite that has weathered to boulders. Black, vesicular lava flows are nearly holohyaline. The few percent of crystals present consist of resorbed plagioclase (0.6 to 2.0 mm, typically 1.2 mm), clinopyroxene (0.3 to 1.0 mm, typically 0.4 mm), hornblende (0.3 mm typically), and iron oxides (0.2 to 0.35 mm)(figure 3). Medium-gray structureless or flow-banded lava flows are also common. They are nearly holohyaline except for plagioclase (0.4 to 1.5 mm, typically 0.6 mm), clinopyroxene (0.3 to 0.8 mm, 0.6 mm typically), and iron oxides (0.16 to 0.28 mm).

A single latite sample was dated for this study. Sample AP19 was collected from Wildcat Hollow and yielded an age of 23.1±1.0 m.y..

Latite samples are from the most silica-rich lava flows of the Awapa Plateau and plot within the trachyte compositional field (figure 4). Sample AP139, from Williams and Hackman's basaltic andesite and latite undifferentiated unit, was reassigned to the latite unit based on its mineralogy and major- and trace-element chemistry.

Definitive correlation of the latite unit away from the Awapa Plateau is difficult. It shares some similarities with several units, including the Antimony Tuff Member of the Mount Dutton Formation (Anderson and Rowley, 1975), the tuff of Albinus Canyon (Steven, 1979; Cunningham and others, 1983; Willis, 1986), and the lava flows of Deer Springs Draw (Nelson, 1989), but differences are significant. Alternatively, the latite unit may be limited to the Awapa Plateau. Both the Antimony Tuff Member and the tuff of Albinus Canyon are beneath the Osiris Tuff, a stratigraphic position similar to the latite unit. Both tuffs are crystal poor, with feldspar being the most common phenocryst, a characteristic shared with the latite. It is possible that these two tuffs were grouped in the latite unit by Williams and Hackman (1971) because of the reconnaissance nature of their mapping. The major- and trace-element chemistry of each unit is distinctive (Mattox, unpublished data; Willis, unpublished data), and unpublished potassium-argon ages (data of H.H. Mehnert in Rowley and others, 1988b) of approximately 25 m.y. show the tuffs are significantly older than the latite. The lava flows of Deer Springs Draw are exposed north of Thousand Lake Mountain and are described by Nelson (1989). These lavas have similarites with the latite flows, including their low abundance of phenocrysts. However, the trachyte lava flows of Deer Spring draw are older (26.3 Ma) and have significant differences in major-element compositions. Field relations between the latite and the other stratigraphic units of the Awapa Plateau clearly demonstrate the relatively thin and laterally discontinuous nature of the latite lava flows. It is possible that the latite was erupted from vents on the Awapa Plateau and, because of its small volume, never extended beyond the plateau's margins. Magmatic centers of similar composition and age occur over a large area of central and western Utah and eastern Nevada (Nelson, 1989).

Osiris Tuff

Williams and Hackman (1971) informally designated the tuff of Osiris for an ash-flow tuff of regional extent. Later work showed the tuff to be the most widespread in the Marysvale field, covering more than 1540 square miles (4000 square km)(Rowley and others, 1986a and b; Rowley and others, 1988a and b; Steven and others, 1984). The tuff is named for exposures near the abandoned village of Osiris, in Black Canyon (sec. 13, T.32S., R.2W.). Anderson and Rowley (1975) formally defined the unit as Osiris Tuff. The Osiris Tuff serves as a stratigraphic marker on the Awapa Plateau, interlayered with and overlying the alluvial facies of the volcanic rocks of Langdon Mountain, and overlying the basaltic andesite and the latite. Excellent exposures can be found in the cliffs of Riley Canyon, where the Osiris Tuff is nearly 200 feet (60 m) thick due to ponding on irregular topography. At other exposures on the plateau, Parker Hollow (sec. 11, T.28S., R.1W.), Long Hollow (NW sec. 19, T.28S., R.2E.), Big Rocks (SW sec. 24, T.28S., R.2E.), and Big Flat Top (sec. 17, T.29S., R.2E.), the ash-flow tuff is 15 to 25 feet (4.5 to 7.6 m) thick and weathers to house-sized boulders. Most exposures contain a black basal vitrophyre a few feet (1 to 2 m) thick overlain by medium-gray welded tuff. The unit contains abundant phenocrysts of plagioclase (0.4 to 2.5 mm, 0.6 mm typically), minor amounts of sanidine (0.5 to 2.5 mm), biotite (0.5 to 2.0 mm, 1.5 mm typically), rare clinopyroxene (0.4 to 1.7 mm), and iron oxides (0.1 to 0.7 mm)(figure 3). The Osiris Tuff is the result of an eruption associated with collapse the Monroe Peak caldera of the northern Sevier Plateau (Steven and others, 1984).

Using samples collected from the southern Tushar Mountains and the Wasatch Plateau the age of the Osiris Tuff is 23 m.y. (Fleck and others, 1975).

Based on chemistry, the Osiris Tuff is a trachyte (figure 4). The considerable chemical variation is probably the result of variable phenocryst and/or lithic abundance, location of the sample within the ash-flow tuff (basal vitrophyre or main body), and the degree of weathering.

Since the informal designation of the tuff of Osiris (Williams and Hackman, 1971) the unit has been mapped throughout the southern High Plateaus (Anderson and others, 1990a and b; Anderson and others, 1981; Cunningham and others, 1983; Rowley and others, 1987; and Willis, 1986). Samples from the Awapa Plateau are petrologically similar to those described at other localities (Anderson and Rowley, 1975, Table 1-1; Rowley and others, 1986b). Ten samples from the type locality of the formation and five samples from other plateaus (Mattox, unpublished data) define a compositional field in figure 5. The Awapa samples plot within or very near the field. Although the Osiris Tuff was not dated on the Awapa Plateau, the isotopic ages of samples AP99 and AP119 constrain its maximum age to 23.2 m.y..

Sevier River Formation

The Sevier River Formation, called volcanic sediments by Williams and Hackman (1971), filled depressions developed on the older stratigraphic units. These unconsolidated, fluvial sediments were derived from surrounding volcanic strata. The formation is well exposed in road cuts in Big Hollow (N sec. 7, T.29S., R.3E.) and near Black Point (N sec. 35, T.27S., R.1E.). At Big Hollow, it has a maximum thickness of about 200 feet (60 m). Laminated, medium grained sandstone, and structureless tuffaceous sandstone comprise most

of the unit. Thick-bedded, tuffaceous, pebbly sandstone and less abundant clast-supported, pebble and cobble conglomerate fill channels that have been eroded in the sandstone. Elsewhere on the plateau, exposures are essentially non-existent and the presence of the unit is marked only by pebbly soil.

The Sevier River Formation of the Awapa Plateau is similar to other exposures on the High Plateaus. Callaghan (1938) designated partly consolidated fanglomerate, conglomerate, sandstone, siltstone, and diatomaceous beds as the Sevier River Formation. The sedimentary rock was derived from local sources and accumulated in nearby basins. Freshwater fauna indicate a late Pliocene or early Pleistocene age for the rocks at the type locality (Callaghan, 1939). Based on the presence of a few outcrops of fluvial sediments in the uplands of the southwestern High Plateaus, Anderson and Rowley (1975, p. 41) thought "it probable that the Sevier River Formation formerly filled significant parts of the intermontane valleys of the southern High Plateaus." On the Awapa Plateau, poorly consolidated sandstone, pebbly sandstone, and clast-supported conglomerate have filled depressions developed on older volcanic rocks. Isotopic ages of 14.2 and 7.1 m.y. were reported by Steven and others (1979) for ash layers at the base and top, respectively, of the Sevier River Formation in the Marysvale area. No datable material was recovered from the Sevier River Formation of the Awapa Plateau but their minimum age is constrained by the overlying olivine basalt (AP26), dated at approximately 16 m.y.

Olivine Basalt

Olivine basalt occurs as lava flows, cinder cones, and volcanic necks. In morphology most individual volcanoes are shields, with central vents still recognizable at Smooth Knoll and Elsies Nipple. Many flows weather to boulders or small, discontinuous outcrops. One exception is the fresh basalt exposed in a road cut at the extreme eastern margin of the plateau (sample AP127)(NWNE sec. 9, T.30S., R.3E.). Maximum thickness of the unit is roughly 450 feet (135 m). Most lava flows consist of black, porphyritic rock dominated by olivine (0.3 to 2.7 mm, typically 1.0 mm), but also contain small crystals of clinopyroxene (0.1 to 0.8 mm. 0.5 mm typically)(figure 3). The olivine commonly weathers to iddingsite. Plagioclase microlites, commonly in a trachytic texture, iron oxides, and volcanic glass make up the groundmass.

Olivine basalts from near the town of Antimony and the southwest rim of the plateau yielded ages from 5.0, 5.4, and 6.6 m.y. (Best and others, 1980). Samples A4 through A7, A2 and A3, and AP142 of this study were collected from the same lava flows, respectively. Two olivine basalt samples were dated for this study. Sample AP26 was collected north of the Awapa Plateau near the southern end of the Fish Lake Plateau. The sample yielded an age of 16.4+/-1.0 m.y.. Sample AP127, collected near the extreme eastern margin of the Awapa Plateau, yielded an age of 5.9+/-0.6 m.y..

Samples from the olivine basalt stratigraphic unit range from basalt to basaltic trachyandesite in composition (figure 4). At some localities in the High Plateaus the young (16 m.y.) basalts cannot be distinguished from older mafic flows because of their similar mineralogy and lack of isotopic age or stratigraphic constraints. All samples of olivine basalt from the Awapa Plateau contain less than 3 weight percent K_2O, suggesting a chemical criterion may be used to differentiate the two stratigraphic units. All of the olivine basalt lava flows are nepheline normative with the exception of the two more evolved samples (AP54 and AP142). Fractional crystallization of the observed phenocryst phases can explain the major-element variation of the

more evolved samples of olivine basalt (figure 7). The more mafic samples are probably related by variable degrees of partial melting of an enriched mantle source (Mattox and Walker, 1990).

The olivine basalt of the Awapa Plateau is part of a widespread sequence of scattered basalts in the High Plateaus (Steven and others, 1990; Cunningham and others, 1983). Dutton (1880) noticed their concentration on the periphery of the Marysvale field. In a detailed study of the mineralogy of the younger basalt flows, Lowder (1973) showed olivine to be the most common phenocryst followed by plagioclase and clinopyroxene. Lava flows of the Awapa Plateau have nearly equal amounts of plagioclase and clinopyroxene. Plagioclase occurs in the groundmass or as phenocrysts. More than 35 samples (Mattox, unpublished data) from younger basalt flows of the Markagunt Plateau and Sevier Plateaus define a field in figure 5. Most lava flows from the Awapa Plateau plot within the field. The higher total alkalies for the more evolved olivine basalts of the Awapa Plateau reflect an eastward increase in these elements for all younger basalt flows of the High Plateaus (Mattox and Walker, 1990). Best and others (1980) reported a range of 0.26 to 12.7 m.y. for younger basalt flows on the Markagunt and Sevier Plateaus. Fleck and others (1975) reported an age of 0.44 m.y. for a flow on the west margin of the High Plateaus. One sample from the southeast margin of the Awapa Plateau yielded an age of 5.9 m.y., very similar to the ages in Best and others (1980). The 16.4 m.y. age for sample AP26 is the oldest reported for a younger basalt flow.

GEOCHEMISTRY

Lavas ranging in composition from basalt to trachyte were erupted on the Awapa Plateau (figure 4). The reader is reminded that eruptive activity was concentrated in two periods, separated by a hiatus of at least 6 million years. Major- and trace-element analyses and CIPW normative calculations are reported in Appendix 2. Major-element and selected trace-element trends are shown in figure 6. With increasing silica, enrichment of Na_2O and K_2O and depletion of CaO, FeO_T, MgO, TiO_2, and P_2O_5 occur. Each stratigraphic unit forms a relatively discrete cluster on the variation diagram for all the elements except Al2O3, which may reflect the variability in the abundance of plagioclase phenocrysts from sample to sample and unit to unit.

The samples define an alkali-lime index (Peacock, 1931) of 56, transitional from alkali-calcic to calc-alkalic. They also appear transitional from alkaline to subalkaline in the alkali-silica plot of Irvine and Barager (1971)(figure 8) but plot well within the subalkaline and calc-alkaline fields of a normative olivine-nepheline-quartz projection and an AFM plot, repectively (Irvine and Baranger, 1971)(figure 9).

The curvilinear pattern on the variation diagrams might reflect crystal fractionation from a single parent or mixing of two magmas with different compositions. Such processes likely acted on the magmas of a single stratigraphic unit (olivine basalt) or several units (andesite breccia, basaltic andesite, and latite) but certainly do not relate the late-Tertiary unit to the mid-Tertiary units.

A chondrite-normalized spider diagram is used to show graphically the variation in trace elements for representative samples from each unit (figure 10). The andesite breccia and the basaltic andesite show similar enrichments and depletions. The chemistry of the latite and the Osiris Tuff suggests that a crustal component may have modified their composition. For example, Zr is

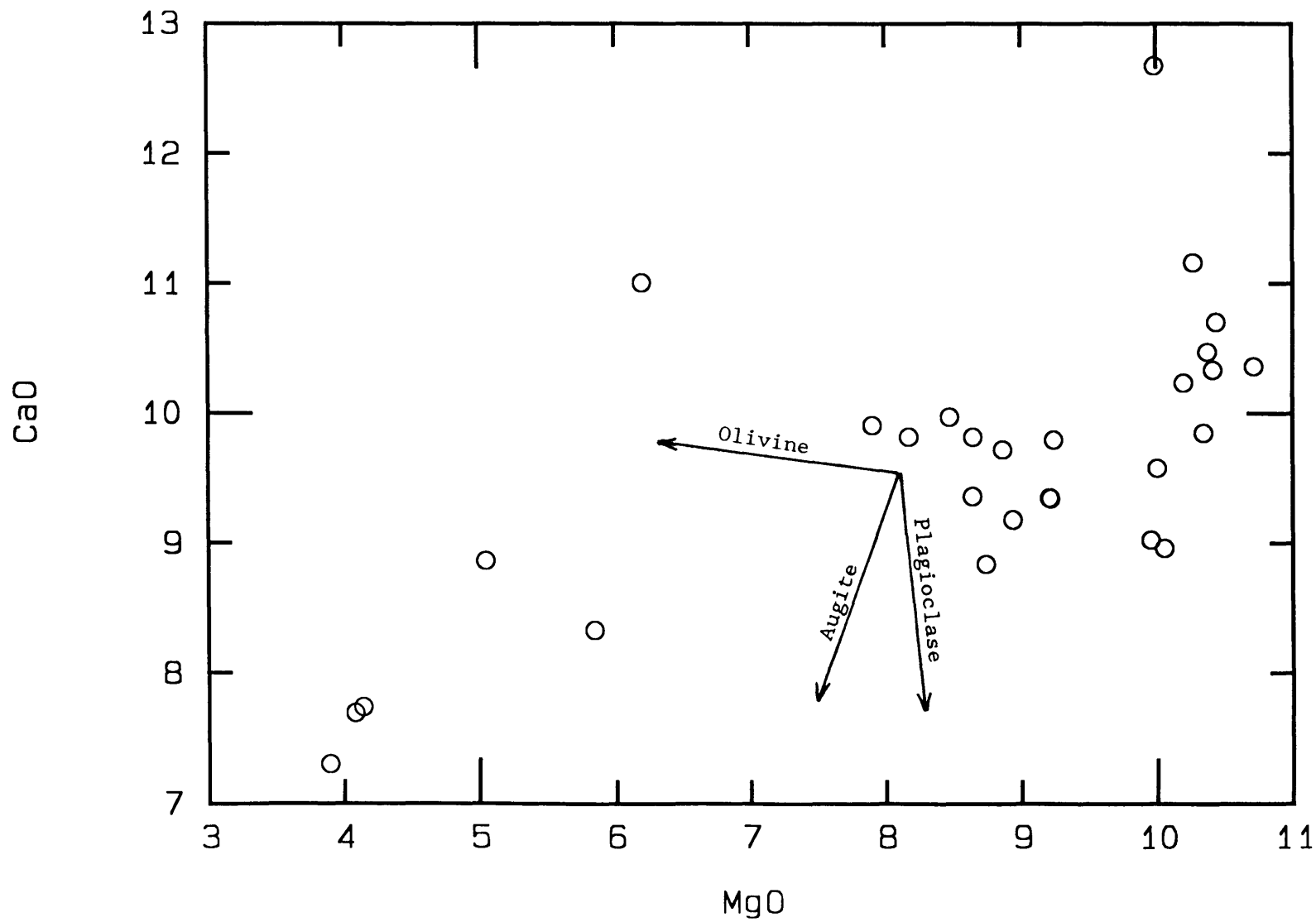

Figure 7. CaO versus MgO content for olivine basalt from the Awapa Plateau. Arrows show control lines for the fractionation of olivine, augite, and plagioclase. The chemistry of the more evolved samples is explained by the fractionation of olivine followed by fractionation of olivine and augite. Both olivine and augite are present in the olivine basalt. Fractionation paths are from Garcia and Wolfe (1988).

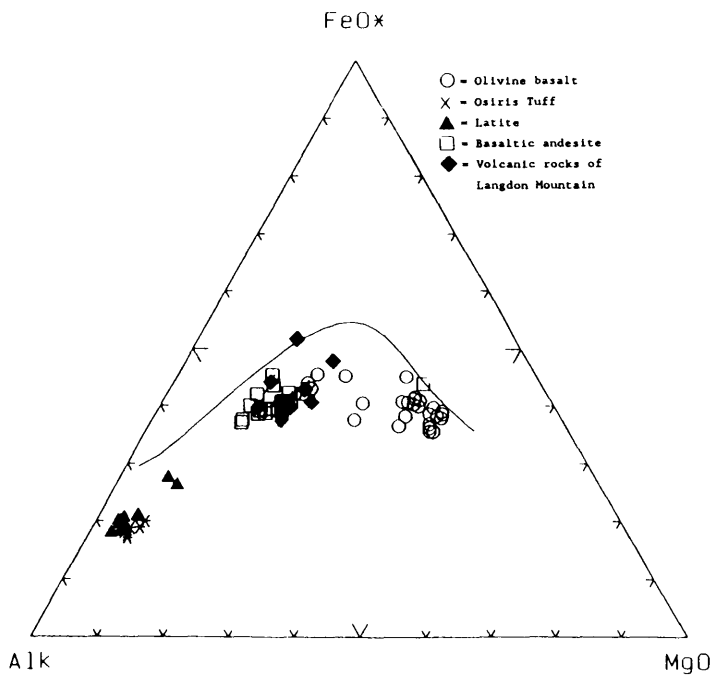

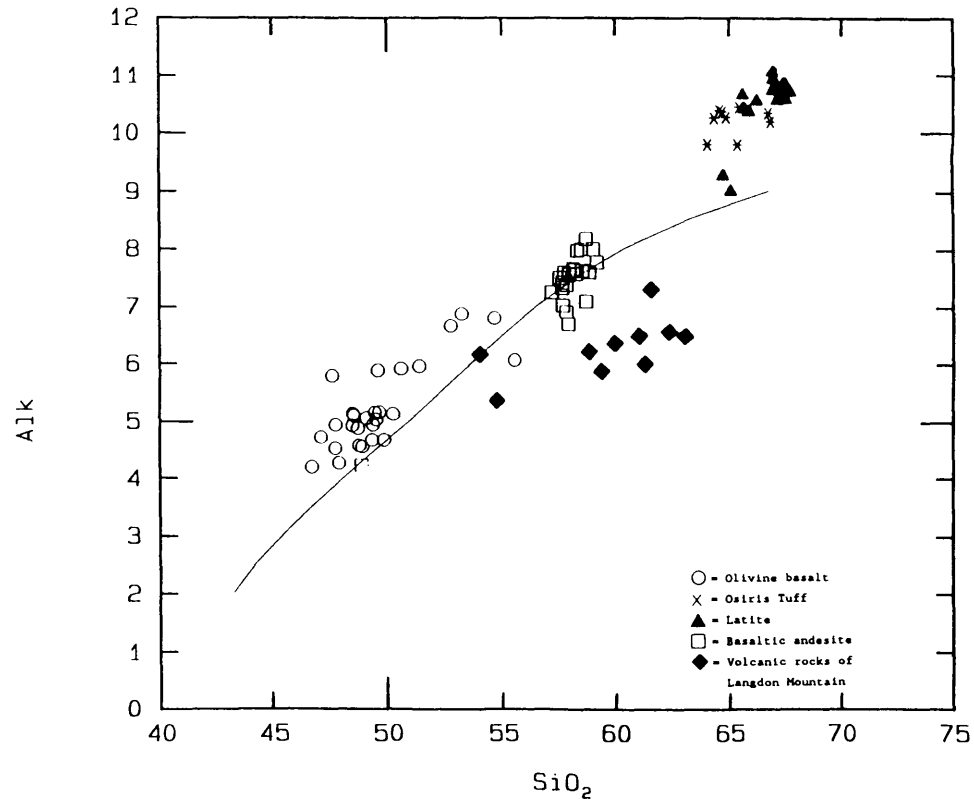

Figure 8. (right). An alkalies - silica plot (Irvine and Barager, 1971), which shows that nearly all samples from the Awapa Plateau are alkaline with the exception of the mudflow breccia clasts. The basaltic andesite appears transitional from subalkaline to alkaline.
Figure 9. (left). An AFM diagram (Irvine and Barager, 1971), showing that samples from the Awapa Plateau display a typical calc-alkaline trend.

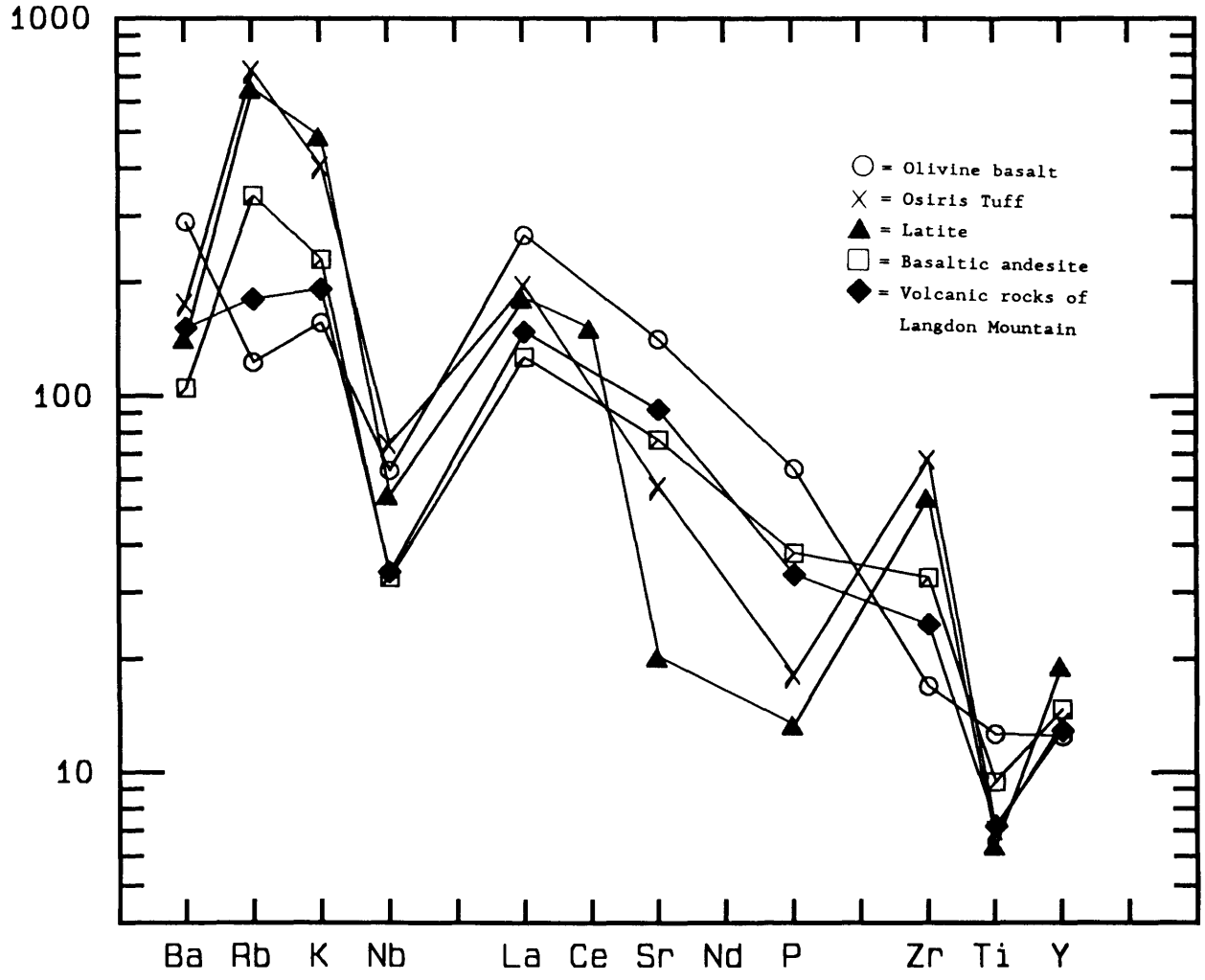

Figure 10. Chondrite-normalized trace-element patterns for representative lavas from each stratigraphic unit.

enriched relative to TiO_2 and P_2O_5, a characteristic of magmas that have been contaminated by crustal rocks (Thompson and others, 1983). All samples have Ba/Nd ratios > 26, a characteristic of subduction-related orogenic lavas (Gill, 1981).

The onset of potassium-rich volcanism is believed by Rowley and others (1988b) to have been coincident with the main phase of structural differentiation of the High Plateaus (Rowley and others, 1978) and the beginning of period of volcanic activity dominated by bimodal, basalt and rhyolite, volcanism. In a detailed study of the geochemistry of middle and late Tertiary rocks from the southern portion of the Marysvale volcanic field, Mattox and Walker (1989) and Mattox (1990) reported systematic enrichments of K_2O and large-ion lithophile elements from middle Tertiary lavas to the potassium-rich lava flows. Late Cenozoic (less than 16 m.y.) lava flows have markedly different chemistry. Mattox and Walker (1989) suggested the enrichment trends may reflect detachment or the demise of a subducted slab beneath the western portion of the continent. A similar compostional trend and tectonic history is reported for the Aeolian Islands by Keller (1974) and Ellam and others (1988). After a hiatus of several million years late Tertiary volcanism began. Selective enrichment in some trace elements indicated that the source of the olivine basalt was modified by CO2-rich, alkaline fluids or magmas (Walker and Mattox, 1989).

GEOLOGIC HISTORY

During the late Oligocene, clastic aprons moved to the east as volcanic mudflows prograded from topographically high stratovolcanoes in the Langdon Mountain area of the northern Sevier Plateau. The presence of lacustrine strata immediately beneath the volcanic sequence suggests the Awapa Plateau area had low relief, facilitating transport of volcanic mudflows to great distances. Deposition continued on the western side of the plateau into the early Miocene. Synchronous with or following shortly after the deposition of the volcanic mudflow breccia, thick flows of basaltic andesite were erupted from vents that are now concealed, removed by erosion, or located to the east. The distribution of the basaltic andesite suggests that it onlapped the mudflow breccia from the east. Alternatively these flows may have traveled from a large shield volcano on the northern Sevier Plateau. In the early Miocene lava flows of the latite unit were erupted from local sources and were interlayered with basaltic andesite lava flows. Mid-Tertiary effusive activity terminated shortly before the deposition of the Osiris Tuff 23 m.y. ago. Variation in the thickness of the Osiris Tuff attests to the irregular topography of the paleosurface. Fluvial deposition began as early as the early middle Miocene, as evidenced by exposures southwest of Fish Lake and the isotopic age of sample AP26, and produced the Sevier River Formation. Olivine basalt was erupted from early middle Miocene to the earliest Pliocene. Activity appears to have peaked in the latest Miocene - earliest Pliocene. Displacement of these young lava flows by the Paunsaugant fault support the relatively recent uplift of the Awapa Plateau noted previously by Rowley and others (1981b).

ACKNOWLEDGEMENTS

Financial support for this project was provided by the Utah Geological and Mineral Survey. Drs. James Walker and Malcolm Weiss of Northern Illinois University and Michael Ross of the Utah Geological and Mineral Survey assisted in the field. Michael Ross collected samples for K-Ar age determination. Mr.

and Mrs. Marion Wankier and Mr. and Mrs. William Rice provided logistical support. Neil Dickey, laboratory technician for the Department of Geology at Northern Illinois University, assisted greatly with both software and hardware problems. Reviews by Drs. Walker and Weiss, Michael Ross, and Peter Rowley of the United States Geological Survey greatly improved this text. Additional assistance was provided by Tari Moulds, Sheri Quesnel, and Richard Markey.

REFERENCES CITED

Anderson, J.J., 1986, Geologic map of the Circleville Mountain quadrangle, Beaver, Piute, Iron, and Garfield Counties, Utah: Utah Geological and Mineral Survey, Map 80.

Anderson, J.J., Iivari, T.A., and Rowley, P.D., 1987, Geologic map of the Little Creek Peak quadrangle, Garfield and Iron Counties, Utah: Utah Geological and Mineral Survey, Map 104.

Anderson, J.J., Lanigan, J.C., Cunningham, C.G., and Naeser, C.W., 1981, Geologic map of the Beaver SE quadrangle, Beaver County, Utah: U.S. Geological Survey Miscellaneous Field Studies Map MF-1274.

Anderson, J.J., and Rowley, P.D., 1975, Cenozoic stratigraphy of southwestern High Plateaus of Utah, in Anderson, J.J., Rowley, P.D., Fleck, R.J., and Nairn, A.E.M., eds., Cenozoic geology of the southwestern High Plateaus of Utah: Geological Society America Special Paper 160, p. 1-51.

Anderson, J.J., and Rowley, P.D., 1987, Geologic map of the Panguitch NW quadrangle, Iron and Garfield Counties, Utah: Utah Geological and Mineral Survey, Map 103.

Anderson, J.J., Rowley, P.D., Machette, M.N., Decatur, S.H., and Mehnert, H.H., 1990a, Geologic map of the Nevershine Hollow area, eastern Black Mountains, southern Tushar Mountains, and northern Markagunt Plateau, Beaver and Iron Counties, Utah: U.S. Geological Survey Miscellaneous Investigations Series Map I-1999, scale 1:50,000.

Anderson, J.J., Rowley, P.D., Blackman, J.T., Mehnert, H.H., and Grant, T.C., 1990b, Geologic map of the Circleville Canyon area, southern Tushar Mountains and northern and Markagunt Plateau, Beaver, Garfield, Iron, and Piute Counties, Utah: U.S. Geological Survey Miscellaneous Investigations Series Map I-2000, scale 1:50,000.

Best, M.G., McKee, E.H., and Damon, P.E., 1980, Space-time-composition patterns of late Cenozoic mafic volcanism, southwestern Utah and adjoining areas: American Journal of Science, v. 280, p. 1035-1050.

Blackman, J.T., 1985, Geology of a vent of the Mount Dutton Formation (Miocene) southwest Tushar mountains, Utah: Kent, Ohio, Kent State University, M.S. thesis, 80 p.

Callaghan, Eugene,1938, Preliminary report on the alunite deposits of the Marysvale region, Utah: U.S. Geological Survey Bulletin 886-D, p. 91-134.

-----1939, Volcanic sequence in the Marysvale region in southwest-central Utah: American Geophysical Union Transactions, 20th Ann. Mtg., Washington, D.C., pt. 3, p. 438-452.

-----1973, Mineral resources potential of Piute County., Utah and adjoining area: Utah Geological and Mineralogical Survey Bulletin 102, 135 p.

Cunningham, C.G., Steven, T.A., Rowley, P.D., Glassgold, L.B., and Anderson, J.J., 1983, Geologic map of the Tushar Mountains and adjoining areas, Marysvale Volcanic field, Utah: U.S. Geological Survey Miscellaneous Investigations Series Map I-1430-A.

Dalrymple, G.B., 1979, Critical tables for conversion of K Ar ages from old to new constants: Geology, v. 7, p. 558 560.

Dutton, C.E., 1880, Report on the geology of the high plateaus of Utah with atlas: U.S. Geographical and Geological Survey, Rocky Mtn. Region (Powell), 307 p.

Ellam, R.M., Menzies, M.A., Hawkesworth, C.J., Leeman, W.P., Rosi, M., and Seri, G., 1988, The transition from calc-alkaline to potassium orogenic magmatism in the Aeolian Islands, souhtern Italy: Bulletin of Volcanology, v. 50, p. 386-398.

Feigenson, M.D., and Carr, M.J., 1985, Determination of major, trace, and rare-earth elements in rocks by DCP-AES, Chemical Geology, v.51, p. 19-27.

Fleck, R.J., Anderson, J.J., and Rowley, P.D., 1975, Chronology of mid-Tertiary volcanism in High Plateaus region of Utah, **in** Anderson, J.J., Rowley, P.D., Fleck, R.J., and Nairn, A.E.M., eds., Cenozoic geology of southwestern High Plateaus of Utah: Geologic Society America Special Paper 160, p. 53-62.

Garcia, M.O., and Wolfe, E.W., 1988, Petrology of lavas, in Wolfe, E.W., ed., The Puu Oo eruption of Kilauea Volcano, Hawaii: Episodes 1 through 20, January 3, 1983, through June 8, 1984: U.S. Geological Survey Professional Paper 1463, 251 p.

Gill, J.B., 1981, Orogenic andesites and plate tectonics: Springer-Verlag, New York, 390 p.

Gladney, E.S., Burns, C.E., and Roelandts, I., 1983, 1982 compilation of elemental concentrations in eleven United States Geological Survey rock standards, Geostandards Newsletter, v. 7, p. 3-226.

Hower, J., 1959, Matrix corrections in the x-ray spectrographic trace element analysis of rocks and minerals, American Mineralogist, v. 44, p. 19-32.

Irvine, T.N., and Baragar, W.R., 1971, A guide to the chemical classification of the common igneous rocks: Canadian Journal Earth Science, v. 8, p. 523-548.

Keller, J., 1974, Petrology of some volcanic rock series of the Aeolian arc, southern Tyrrhenian Sea: calc-alkaline and shoshonitic associations: Contibutions to Mineralogy and Petrology, v. 46, p. 29 47.

Kennedy, R.R., 1963, Geology of Piute County, Utah: Tucson, University of Arizona, Ph.D. thesis, 282 p.

Le Bas, M.J., Le Maitre, R.W., Streckeisen, A., and Zanettin, B., 1986, A chemical classification of volcanic rocks based on the total alkali-silica diagram: Journal of Petrology, v. 27, 745-750.

Lowder, G.G., 1973, Late Cenozoic transitional alkali olivine-tholeiitic basalt and andesite from the margin of the Great Basin, southwest Utah: Geological Society America Bulletin, v. 84, p. 2993-3012.

Mattox, S.R., 1990, Volcanic history of the Awapa Plateau, south-central Utah: Geological Society America Abstract with Programs, v. 22, p. 65.

Mattox, S.R., and Walker, J.A., 1989, Geochemistry and tectonism of lavas erupted during the transition from compression to extension, southern Marysvale complex, southwestern Utah: IAVCEI Abst., New Mexico Bureau of Mines & Mineral Resources, Bulletin 131, p. 178.

-----1990, Late Cenozoic lavas of the Utah Transition Zone: Geological Society America Abstract with Programs, v. 22, p. 65.

Nelson, S.T., 1989, Geologic map of the Geyser Peak quadrangle, Wayne and Sevier Counties, Utah: Utah Geological and Mineral Survey Map 114.

Palmer, B.A., and Walton, A.W., 1990, Accumulation of volcaniclastic aprons in the Mount Dutton Formation (Oligocene-Miocene), Marysvale volcanic field, Utah: Geological Society America Bulletin, v. 102, p. 734-748.

Peacock, M.A., 1931, Classification of igneous rock series: Journal Geology, v. 39, p. 54-67.

Rowley, P.D.,1979, Geologic map of the Marysvale SE quadrangle, Piute County, Utah: U.S. Geological Survey Miscellaneous Field Studies Map MF 115, scale 1:24,000.

Rowley, P.D., Anderson, J.J., Williams, P.L., Fleck, R.J., 1978, Age of structural differentiation between the Colorado Plateau and Basin and Range provinces in southwestern Utah: Geology, v. 6, p. 51-55.

Rowley, P.D., Cunningham, C.G., Steven, T.A., Mehnert, H.H., and Naeser, C.W., 1988a, Geologic map of the Marysvale quadrangle, Piute County, Utah: Utah Geological & Mineral Survey Map 105.

-----1988b, Geologic map of the Antelope Range quadrangle, Sevier and Piute Counties, Utah: Utah Geological and Mineral Survey Map 106.

Rowley, P.D., Hereford, R., and Willams, V.S., 1987, Geologic map of the Adams Head - Johns Valley area, southern Sevier Plateau, Garfield county, Utah: U.S. Geological Survey Miscelllaneous Investigations Series Map I-1798.

Rowley, P.D., Steven, T.A., Anderson, and Cunningham, C.G., 1979, Cenozoic stratigraphic and structural framework of southwestern Utah: U.S. Geological Survey Professional Paper 1149, 22 p.

Rowley, P.D., Steven, T.A., Mehnert, H.H., 1981, Origin and structural implications of upper Miocene rhyolites in Kingston Canyon, Piute County, Utah: Geological Society of America Bulletin, v. 92, p. 590-602.

Rowley, P.D., Williams, P.L., and Kaplan, A.M., 1986a, Geologic map of the Greenwich quadrangle, Piute County, Utah: U.S. Geological Survey Geologic Quadrangle Map GQ-1589.

Rowley, P.D., Willams, P.L., and Kaplan, A.M., 1986b, Geologic map of the Koosharem quadrangle, Sevier and Piute Counties, Utah: U.S. Geological Survey Geologic Quadrangle Map GQ-1590.

Smith, J.F., Jr., Huff, L.C., Hinrichs, E.N., and Luedke, R.G., 1963, Geology of the Capitol Reef area, Wayne and Garfield Counties, Utah: U.S. Geological Survey Professional Paper 363, 102 p.

Steiger, R.H., and Jager, E., 1977, Subcommission on geochronology: Convention on the use of decay constants in geo- and cosmochronology: Earth and Planetary Science Letters, v. 36, p. 359-362.

Steven, T.A., 1979, Geologic map of the Monroe NW quadrangle, west central Utah: U.S. Geological Survey Miscellaneous Field Studies Map MF 1107, scale 1:24,000.

Steven, T.A., Cunningham, C.G., Naeser, C.W., and Mehnert, H.H., 1979, Revised stratigraphy and radiometric ages of volcanic rocks in the Marysvale area, west-central Utah: U.S. Geological Survey Bulletin 1469, 40 p.

Steven, T.A., Morris, H.T., and Rowley, P.D., 1990, Geologic map of the Richfield 1 degree x 2 degree quadrangle, west-central Utah: U.S. Geological Survey Miscellaneous Investigations Series Map I-1901.

Steven, T.A., Rowley, P.D., and Cunningham, C.G., 1984, Calderas of the Marysvale Volcanic Field, west central Utah: Journal Geophysical Research, v. 89, p. 8751-8764.

Thompson, R.N., Morrison, M.A., Dickin, A.P., and Hendry, G.L., 1983, Continental flood basalts and mantle xenoliths ... Arachnids Rule OK? in Hawkesworth, C.J., and Norry, M.J., eds., Continental basalts and mantle xenoliths: Shiva, p. 158-185.

Walton, A.W., and Palmer, B.A., 1988, Lahar facies of the Mount Dutton Formation (Oligocene-Miocene) in the Marysvale Volcanic Field, southwestern Utah: Geological Society America Bulletin, v. 100, p. 1078-1091.

Willams, P.L., and Hackman,R.J., 1971, Geology, structure, and uranium deposits of the Salina quadrangle, Utah: U.S. Geological Survey Miscellaneous Geologic Investigations Map I-591.

Willis, G., 1986, Geologic map of the Salina quadrangle, Sevier County, Utah: Utah Geological and Mineral Survey map 83.

Willis, G., unpublished, Guide to accompany the field trip through Salina quadrangle, Sevier County, Utah June 28, 1984.

Walker, J.A., and Mattox, S.R., 1989, The influences of subduction on mid-late Cenozoic volcanism in southwestern Utah: Geological Society of America Abstracts with Programs, v. 21, p. A57.

APPENDIX 1
SAMPLE LOCATIONS

Sample	Unit	Longitude	Latitude	7.5' quadrangle	Locality
AP36	Tla	111°52'56"	38°20'54"	Parker Knoll	N of Cinco
AP37	"	"	"	"	"
AP38	"	"	"	"	"
AP40	"	111°53'55"	39°19'30"	"	Dog Lake
AP41	"	"	"	"	"
AP42	"	"	"	"	"
AP65	"	111°44'45"	38°18" 7"	Moroni Peak	Cyclone Draw
AP66	"	"	"	"	"
AP67	"	"	"	"	"
AP72	"	111°45' 5"	38°15'18"	Jakes Knoll	Bull Roost
AP92	"	111°52'46"	38°24'20"	Greenwich	Parker Springs
AP93	"	"	"	"	"
AP19	Tba	111°39'27"	38°25' 0"	Loa	NW of Loa
AP21[1]	"	111°49'19"	38°29' 3"	Abes Knoll	on Highway 25
AP24[1]	"	111°49 3"	38°29' 4"	"	"
AP27[1]	"	111°45'51"	38°30'13"	Burrville	S of Fish Lake[2]
AP28[1]	"	"	"	"	"
AP47[1,3]	"	111°49'51"	38° 9'22"	Flossie Knoll	E of the Tanks
AP75[4]	"	111°39'42"	38°12'22"	Smooth Knoll	Wildcat Hollow
AP84[4]	"	111°40'21"	38°24'30"	Loa	W of Loa
AP87	"	111°38'39"	38°25'30"	"	Alfred Point
AP96	"	111°46'37"	38°24'48"	Abes Knoll	Black Point
AP98	"	111°46'43"	38°24'52"	"	"
AP99[5]	"	111°46'42"	38°23'35"	"	Eightmile Res.
AP104	"	111°43'41"	38°22' 4"	Moroni Peak	Long Hollow
AP105	"	111°42'47"	38°21'59"	"	"
AP111	"	111°36'38"	38°21' 1"		airport
AP114	"	111°33'54"	38°17'17"	Bicknell	Bicknell Bottoms
AP125	"	111°35'51"	38°14' 3"	Government Point	Giles Hollow
AP126[6]	"	"	"	"	"
AP136[1]	"	111°49'37"	38° 6' 1"	Pollywog Lake	SW of Pollywog L
AP145	"	111°27'47"	38°26' 2"	Torrey	Thousand L Mtn
AP146	"	111°27'43"	38°25'23"	"	"
AP15	Tl	111°41'44"	38°12'50"	Smooth Knoll	Balsam Hollow
AP60	"	111°38'13"	38°17'48"	Moroni Peak	Big Hollow, base
AP62	"	111°38'14"	38°17'45"	"	"
AP63	"	111°38'15"	38°17'44"	"	Big Hollow, top
AP69	"	111°42'40"	38°17'21"	"	S of Big Flat T
AP115	"	111°35' 4"	38°17'15"	Bicknell	Bicknell Bottoms
AP116	"	"	"	"	"
AP119[7]	"	111°38'47"	38°14'28"	Smooth Knoll	Wildcat Hollow
AP120	"	"	"	"	"
AP121	"	"	"	"	"
AP122	"	"	"	"	"
AP139[1]	"	111°49'34"	38° 5'54"	Pollywog Lake	SW of Pollywog L

AP64	Tlo	111°43′ 5"	38°17′10"	Moroni Peak	Big Flat Top
AP90	"	111°52′33"	38°24′21"	Greenwich	Parker Springs
AP91v[8]	"	"	"	"	"
AP100	"	111°46′42"	38°23′35"	Abes Knoll	Eightmile Res
AP101v	"	111°44′28"	38°22′ 4"	Moroni Peak	Long Hollow
AP102	"	"	"	"	"
AP103	"	"	"	"	"
AP110	"	111°37′22"	38°21′49"	Bicknell	Big Rock
AP140v	"	111°49′34"	38° 5′57"	Pollywog Lake	SW of Pollywog L
AP6	QTb	111°50′ 5"	38°18′23"	Jakes Knoll	Red Knoll
AP8	"	111°52′ 9"	38°15′14"	"	Parker Knoll
AP9	"	"	38°11′34"	Flossie Knoll	no name
AP10	"	111°50′46"	38° 9′ 5"	"	The Tanks
AP25	"	111°47′45"	38°45′53"	Burrville	roadcut
AP26[9]	"	111°47′54"	38°45′ 5"	"	NW of Hw 25
AP32	"	111°49′27"	38°26′22"	Abes Knoll	NE of Abes Knoll
AP33	"	111°50′49"	38°25′33"	"	Abes Knoll
AP45	"	111°50′11"	38°12′50"	Flossie Knoll	Middle Butte
AP52	"	111°48′13"	38° 8′57"	"	Burnt Knoll
AP54	"	111°46′38"	38°11′46"	"	Bald Knoll
AP55	"	111°46′48"	38°11′53"	"	Cedar Peak
AP58	"	111°48′22"	38°14′ 6"	"	Flossie Knoll
AP76	"	111°40′35"	38°10′21"	Smooth Knoll	Smooth Knoll
AP78	"	111°41′ 0"	38° 7′36"	"	Timbered Knoll
AP80	"	111°41′38"	38° 5′ 4"	Big Lake	Big Lake
AP107	"	111°41′41"	38°20′10"	Moroni Peak	Elsies Nipple
AP127[10]	"	111°35′ 8"	38°13′48"	Government Point	Lookout Pk Rd
AP131	"	111°37′28"	38°19′22"	Bicknell	lower Big Hollow
AP133	"	111°48′51"	38° 6′18"	Pollywog Lake	NE of Pollywog L
AP142	"	111°53′21"	38° 9′18"	Angle	W of the Tanks[11]
AP143	"	"	"	"	"
A1	"	111°57′23"	38° 7′20"	Antimony	Antimony Wash
A2	"	111°57′40"	38° 8′00"	Angle	N of Dry Wash[12]
A3	"	"	"	"	"
A4	"	111°59′36"	38°09′57"	"	N of Antimony
A5	"	"	"	"	"
A6	"	111°59′38"	38° 9′45"	"	"
A7[13]	"	"	"	"	"

[1]= mapped as Tla by Williams and Hackman (1971)
[2]= sample hpl-3 of Best and others (1980), age = 24.5 0.5 Ma
[3]= age = 25.2 1.6 Ma
[4]= mapped as Tl by Williams and Hackman (1971)
[5]= age = 23.2 1.5 Ma
[6]= age = 25.8 1.4 Ma
[7]= age = 23.1 1.0 Ma
[8]= v = basal vitophyre
[9]= age = 16.4 1.0 Ma
[10] = age = 5.9 0.6 Ma
[11] = sample hpl-4 of Best and others (1980), age = 6.5 0.3 Ma
[12] = sample hpl-5 of Best and others (1980), age = 5.4 0.4 Ma
[13] = sample pan-27 of Best and others (1980), age = 5.0 0.3 Ma

APPENDIX 2

MAJOR- AND TRACE-ELEMENT CHEMISTRY AND CIPW NORMATIVE COMPOSITIONS

Volcanic rocks of Langdon Mountain

Sample	AP36	AP37	AP38	AP40	AP41	AP42	AP65	AP66
SiO_2	59.90	58.13	59.17	53.76	52.99	58.66	61.44	57.02
TiO_2	0.74	0.86	0.76	1.09	1.25	0.77	0.65	0.75
Al_2O_3	15.85	15.23	16.70	16.87	17.44	16.46	15.51	15.32
FeO	6.05	7.02	6.36	8.40	9.37	6.65	5.55	6.21
MnO	0.14	0.14	0.14	0.16	0.13	0.14	0.12	0.13
MgO	2.83	3.84	2.96	3.95	2.67	3.19	2.11	3.02
CaO	5.81	6.53	5.64	8.11	7.63	6.57	5.28	5.92
Na_2O	3.63	3.57	3.51	3.24	3.52	3.27	3.79	3.46
K_2O	2.76	2.58	2.76	2.03	2.49	2.44	2.52	2.61
P_2O_5	0.35	0.37	0.35	0.39	0.55	0.35	0.29	0.36
LOI	1.54	1.21	1.43	1.18	1.10	1.23	0.98	1.23
Total	99.60	99.48	99.78	99.18	99.14	99.73	98.24	96.03
V	115.6	132.5	115.0	202.8	242.4	127.8	102.6	118.5
Sc	11.1	16.5	14.2	23.7	23.6	13.1	16.2	17.3
Ba	1039.8	925.2	1014.1	836.3	867.5	1025.7	1076.6	916.0
La	48.2	45.6	42.8	45.6	60.0	43.7	33.6	36.6
Ce	0.0	0.0	92.4	0.0	96.8	0.0	0.0	0.0
Cr	51.5	97.6	52.0	26.8	21.1	206.2	34.6	34.9
Co	56.6	32.4	30.3	40.8	31.9	35.9	30.8	32.3
Ni	16.3	25.2	17.6	13.5	13.8	54.6	14.0	13.8
Cu	22.7	26.4	37.0	47.9	50.4	25.7	32.4	21.7
Zn	94.7	88.3	80.3	93.2	86.0	78.6	64.2	78.6
Ga	21.9	20.2	19.4	22.1	22.6	22.6	20.2	18.8
Pb	24.3	21.3	56.3	14.7	28.5	23.7	19.7	18.6
Th	9.9	6.7	8.1	8.6	5.7	11.7	7.5	7.2
Rb	62.8	60.5	59.8	40.3	53.1	54.8	52.9	63.8
Sr	1076.6	1057.6	1125.8	997.9	1206.4	1117.3	1107.4	1011.6
Y	25.7	27.7	27.4	31.9	40.5	25.7	19.0	24.6
Zr	167.8	167.0	198.7	140.2	227.5	135.7	122.4	148.6
Nb	11.8	11.5	10.4	7.0	11.0	9.9	9.7	10.4
Q	9.6	6.1	8.7	1.3	0.0	8.9	13.2	7.8
or	16.3	15.3	16.3	12.0	14.7	14.4	14.9	15.4
ab	30.7	30.2	29.7	27.4	29.8	27.7	32.1	29.3
an	18.8	17.9	21.7	25.5	24.4	23.0	17.9	18.6
di	6.5	10.1	3.4	10.2	8.4	6.1	5.4	7.1
hy	13.9	16.3	16.4	18.6	15.1	16.1	11.9	14.4
ol	0.0	0.0	0.0	0.0	2.0	0.0	0.0	0.0
il	1.4	1.6	1.4	2.1	2.4	1.5	1.2	1.4
ap	0.8	0.9	0.8	0.9	1.3	0.8	0.7	0.8

	Langdon Mountain				Basaltic Andesite			
Sample	AP67	AP72	AP92	AP93	AP19	AP21	AP24	AP27
SiO_2	60.25	40.07	61.56	60.06	56.32	57.06	55.26	57.64
TiO_2	0.72	2.30	0.93	0.85	1.01	1.04	1.03	1.04
Al_2O_3	16.93	12.55	14.44	13.59	15.32	16.11	15.45	15.90
FeO	6.33	16.21	6.58	6.16	7.22	6.85	6.82	6.98
MnO	0.10	0.18	0.12	0.09	0.12	0.13	0.12	0.12
MgO	2.13	10.33	3.38	3.10	3.27	2.36	3.19	3.39
CaO	5.71	11.48	5.54	5.49	5.91	5.17	5.73	5.88
Na_2O	3.52	2.15	3.87	3.78	3.68	3.97	3.72	3.93
K_2O	2.45	0.99	3.45	2.52	3.75	3.96	3.47	3.61
P_2O_5	0.27	1.26	0.37	0.37	0.50	0.49	0.51	0.48
LOI	1.05	0.52	1.17	1.48	2.85	1.21	1.20	0.71
Total	99.46	98.04	101.41	97.49	99.95	98.35	96.50	99.68
V	106.1	576.7	139.9	123.9	146.0	173.7	167.3	172.5
Sc	12.5	62.6	14.3	15.8	11.4	17.7	14.5	17.1
Ba	914.9	443.7	962.7	930.4	890.3	969.0	969.0	938.1
La	31.3	36.4	51.4	37.7	39.0	57.0	43.3	54.3
Ce	73.7	0.0	0.0	0.0	0.0	0.0	0.0	0.0
Cr	33.6	105.4	172.1	147.8	26.4	29.5	30.3	27.4
Co	24.5	73.8	37.4	31.2	23.0	26.3	29.7	38.6
Ni	14.5	62.0	60.9	60.8	17.9	21.5	24.0	16.8
Cu	26.8	38.4	47.1	45.9	92.4	106.4	101.4	98.5
Zn	60.2	132.7	70.5	66.9	76.7	79.0	87.5	86.2
Ga	19.9	24.1	21.6	20.5	18.7	24.0	23.3	21.0
Pb	20.5	0.2	30.4	15.5	34.1	43.8	35.5	29.3
Th	8.6	3.6	12.1	9.0	19.9	20.6	19.2	23.0
Rb	58.1	8.3	102.4	57.7	113.1	142.0	105.9	113.8
Sr	957.8	842.5	1004.8	998.6	1033.3	1089.8	1086.2	1117.0
Y	23.6	44.1	25.6	20.5	26.3	36.8	28.2	26.9
Zr	177.6	73.2	213.8	135.2	206.6	237.8	229.4	232.5
Nb	10.3	7.3	10.5	10.4	10.6	12.8	12.3	13.1
Q	11.6	0.0	7.9	11.1	7.0	2.3	1.9	1.9
or	14.5	0.0	20.4	14.9	22.2	23.4	20.5	21.3
ab	29.8	0.0	32.8	32.0	31.1	33.6	31.5	33.3
an	23.2	0.0	11.8	12.7	14.2	14.4	15.2	15.1
di	2.9	0.0	11.0	10.1	6.8	6.8	8.3	9.1
hy	14.5	0.0	13.7	12.7	5.0	13.6	14.9	15.2
il	1.4	0.0	1.8	1.6	0.3	2.0	2.0	2.0
hem	0.0	0.0	0.0	0.0	7.2	0.0	0.0	0.0
ti	0.0	0.0	0.0	0.0	2.2	0.0	0.0	0.0
ap	0.6	0.0	0.9	0.9	1.2	1.1	1.2	1.1

	Basaltic Andesite							
Sample	AP28	AP47	AP75	AP84	AP87	AP96	AP98	AP99
SiO_2	59.18	56.56	55.72	57.04	64.09	57.62	58.46	58.30
TiO_2	1.06	0.83	0.94	1.02	0.75	1.09	1.05	1.12
Al_2O_3	16.64	18.01	16.76	16.03	16.78	16.10	15.98	15.83
FeO	6.98	5.61	7.17	6.92	3.74	7.35	6.98	7.47
MnO	0.12	0.12	0.12	0.14	0.09	0.13	0.12	0.13
MgO	2.79	2.09	3.17	2.86	0.99	3.43	3.25	3.33
CaO	5.76	6.11	5.95	5.47	2.88	6.28	5.87	5.77
Na_2O	4.04	4.06	3.76	3.99	3.67	3.85	3.88	3.87
K_2O	4.03	3.38	3.48	3.79	5.18	3.55	3.72	3.69
P_2O_5	0.51	0.44	0.37	0.49	0.27	0.47	0.49	0.49
LOI	1.11	0.38	0.72	0.44	1.54	0.97	0.67	0.85
Total	102.22	97.59	98.16	98.19	99.98	100.84	100.47	100.85
V	166.5	132.7	160.1	172.6	53.6	212.1	169.5	210.5
Sc	13.7	13.5	14.2	13.1	9.5	16.8	16.5	13.4
Ba	1063.2	719.9	679.2	964.9	779.0	1002.1	1002.4	947.5
La	52.9	48.3	43.3	52.1	52.4	53.6	51.8	60.6
Nd	0.0	45.5	0.0	0.0	0.0	0.0	0.0	0.0
Ce	0.0	91.7	0.0	0.0	0.0	0.0	0.0	0.0
Cr	27.7	18.4	43.5	31.9	4.9	62.6	38.2	37.5
Co	37.5	26.3	26.8	28.7	32.8	62.1	32.5	38.9
Ni	21.3	11.8	19.7	18.4	5.9	30.0	16.9	18.1
Cu	110.3	114.6	117.5	106.4	31.2	98.6	99.9	105.6
Zn	87.3	67.5	77.1	77.4	64.5	95.9	83.0	93.9
Ga	22.5	23.4	22.6	24.9	21.0	22.1	21.9	23.2
Pb	37.8	32.4	30.7	56.7	58.5	31.4	38.7	36.7
Th	23.4	16.1	17.9	21.6	27.4	22.7	21.1	19.1
Rb	132.6	91.7	102.6	132.9	196.3	102.4	122.1	123.0
Sr	1186.6	965.4	847.4	1109.0	442.9	1172.8	1143.9	1137.8
Y	30.9	26.6	26.5	28.7	35.0	28.1	28.5	28.5
Zr	241.8	173.8	204.5	230.9	371.9	220.4	235.3	240.4
Nb	13.5	10.5	13.3	12.4	17.5	13.2	14.6	12.7
Q	2.2	2.3	0.6	1.6	13.4	1.5	2.8	2.5
or	23.8	20.0	20.6	22.4	30.6	21.0	22.0	21.8
ab	34.2	34.3	31.8	33.8	31.0	32.6	32.8	32.8
an	15.4	20.9	18.6	14.6	12.5	16.2	15.2	14.9
C	0.0	0.0	0.0	0.0	0.6	0.0	0.0	0.0
di	8.3	5.5	7.2	7.8	0.0	10.0	9.0	8.8
hy	14.1	11.6	16.1	14.5	8.3	15.5	14.9	16.0
il	2.0	1.6	1.8	1.9	1.4	2.1	2.0	2.1
ap	1.2	1.0	0.9	1.1	0.6	1.1	1.1	1.1

	Basaltic Andesite							
Sample	AP104	AP105	AP111	AP114	AP125	AP126	AP136	AP145
SiO_2	58.33	58.37	56.78	56.16	56.73	57.92	56.88	57.50
TiO_2	0.99	1.00	1.01	0.94	1.03	0.97	0.85	0.99
Al_2O_3	15.98	16.37	16.53	16.80	16.39	17.07	19.35	15.99
FeO	6.61	6.64	6.82	7.24	7.68	7.21	5.70	7.49
MnO	0.12	0.11	0.13	0.12	0.13	0.13	0.11	0.14
MgO	2.84	2.68	3.01	3.20	2.73	3.43	2.09	3.68
CaO	5.50	5.30	6.08	5.89	5.66	6.16	5.99	6.39
Na_2O	3.91	3.98	3.81	3.65	3.60	3.73	3.93	3.50
K_2O	3.73	3.91	3.64	3.52	3.62	3.30	3.47	3.13
P_2O_5	0.46	0.46	0.47	0.38	0.43	0.40	0.41	0.39
LOI	1.31	1.24	1.42	1.02	1.08	0.92	0.72	0.82
Total	99.78	100.06	99.70	98.92	99.08	101.24	99.50	100.02
V	161.9	161.5	157.8	166.9	185.0	181.1	123.0	176.1
Sc	12.6	15.8	16.8	18.0	16.3	14.1	10.8	18.7
Ba	970.9	998.8	954.4	676.7	696.8	720.0	734.5	742.2
La	46.5	49.3	51.9	44.0	45.6	41.3	47.2	40.8
Ce	0.0	0.0	96.6	0.0	0.0	0.0	0.0	0.0
Cr	44.8	57.8	37.4	31.6	37.2	32.3	23.4	31.6
Co	31.1	25.3	32.5	33.1	32.8	32.8	21.8	34.0
Ni	17.8	15.9	19.6	17.6	22.9	18.7	11.8	19.4
Cu	102.5	102.6	101.6	112.8	133.5	139.3	97.6	130.4
Zn	82.3	80.7	75.9	75.1	81.7	78.7	62.8	85.1
Ga	21.4	21.8	20.5	21.0	20.8	24.5	20.9	23.0
Pb	38.2	48.0	40.9	32.4	47.7	35.9	30.0	32.6
Th	22.0	19.5	21.4	17.2	18.2	19.4	14.8	15.2
Rb	132.4	133.5	92.1	113.5	134.2	117.8	89.2	114.8
Sr	1143.6	1121.4	1173.4	845.7	802.6	893.7	887.6	750.0
Y	27.9	25.5	27.3	27.1	31.9	29.2	26.6	29.9
Zr	228.1	225.2	239.5	206.2	238.4	223.3	162.2	221.9
Nb	13.9	12.5	11.9	11.5	13.0	11.4	11.0	11.7
Q	3.7	3.0	1.6	1.4	2.8	2.7	2.2	3.7
or	22.0	23.1	21.5	20.8	21.4	19.5	20.5	18.5
ab	33.1	33.7	32.2	30.9	30.5	31.6	33.3	29.6
an	15.0	15.3	17.3	19.1	17.9	20.1	24.9	18.7
di	7.8	6.8	8.3	6.4	6.3	6.6	1.8	8.8
hy	13.9	14.0	14.4	16.7	16.3	17.1	13.6	17.2
il	1.9	1.9	1.9	1.8	2.0	1.8	1.6	1.9
ap	1.1	1.1	1.1	0.9	1.0	0.9	0.9	0.9

	Basaltic Andesite		Latite					
Sample	AP146	Smith4	AP15	AP60	AP62	AP63	AP69	Smith8
SiO_2	56.21	58.70	66.66	65.50	66.11	66.51	64.57	65.60
TiO_2	0.97	1.00	0.66	0.66	0.67	0.68	0.83	0.72
Al_2O_3	16.08	17.00	16.80	15.58	15.93	15.56	16.29	16.60
FeO	7.57	7.98	2.50	2.67	2.57	2.79	3.77	2.97
MnO	0.15	0.12	0.08	0.05	0.12	0.10	0.09	0.05
MgO	3.20	2.53	0.47	0.58	0.56	0.58	1.33	0.84
CaO	6.35	4.95	1.19	1.35	1.41	1.38	3.29	2.20
Na_2O	3.64	3.33	4.02	4.35	4.33	4.40	4.22	4.00
K_2O	3.25	3.74	6.98	6.17	6.37	6.27	5.01	6.30
P_2O_5	0.36	0.57	0.14	0.15	0.14	0.16	0.30	0.18
LOI	1.01	0.00	1.23	0.93	1.57	0.48	1.85	0.00
Total	98.79	99.92	100.73	97.99	99.78	98.91	101.55	99.46
V	209.0	0.0	39.7	24.1	23.6	27.1	47.9	0.0
Sc	18.1	0.0	8.4	10.0	5.2	6.9	10.6	0.0
Ba	744.0	0.0	973.1	936.1	900.1	897.6	870.5	0.0
La	48.7	0.0	59.1	51.5	59.0	53.7	60.8	0.0
Ce	0.0	0.0	129.8	0.0	0.0	0.0	0.0	0.0
Cr	39.4	0.0	70.7	114.5	1.8	191.0	9.9	0.0
Co	35.7	0.0	23.9	13.4	14.9	14.6	24.4	0.0
Ni	21.6	0.0	13.2	8.3	4.1	9.2	6.6	0.0
Cu	126.1	0.0	12.6	12.6	12.0	16.1	16.3	0.0
Zn	78.4	0.0	51.5	53.6	49.6	56.1	69.0	0.0
Ga	25.7	0.0	16.9	20.0	18.3	19.7	19.6	0.0
Pb	57.9	0.0	92.7	44.4	54.4	68.2	57.0	0.0
Th	14.9	0.0	33.4	34.8	32.9	33.4	31.0	0.0
Rb	117.0	0.0	226.5	233.4	224.7	237.0	200.4	0.0
Sr	771.9	0.0	236.4	246.8	245.1	244.1	482.1	0.0
Y	29.9	0.0	37.9	35.5	33.6	36.7	33.2	0.0
Zr	216.9	0.0	363.2	403.8	380.8	424.1	398.4	0.0
Nb	12.9	0.0	18.9	17.7	18.0	19.7	20.9	0.0
Q	1.9	6.3	12.0	11.7	11.5	12.0	10.9	11.0
or	19.2	22.1	41.3	36.5	37.7	37.0	29.6	37.2
ab	30.8	28.2	34.0	36.8	36.6	37.2	35.7	33.8
an	17.9	20.4	5.0	4.8	5.2	4.2	10.7	8.7
C	0.0	0.0	0.8	0.0	0.0	0.0	0.0	0.0
di	9.4	0.4	0.0	0.8	0.7	1.4	3.1	0.9
hy	15.8	19.3	4.8	4.9	4.8	4.9	7.5	6.0
il	1.8	1.9	1.3	1.3	1.3	1.3	1.6	1.4
ap	0.8	1.3	0.3	0.3	0.3	0.4	0.7	0.4

	Latite							
Sample	Smith9	AP115	AP116	AP119	AP120	AP121	AP122	AP139
SiO_2	64.10	66.99	64.88	65.37	67.53	66.19	66.55	65.86
TiO_2	0.72	0.68	0.66	0.73	0.69	0.67	0.67	0.71
Al_2O_3	16.00	16.71	16.30	15.57	17.08	15.69	16.92	17.00
FeO	2.90	2.53	2.44	2.91	2.60	2.73	2.55	2.57
MnO	0.06	0.07	0.07	0.08	0.06	0.08	0.06	0.06
MgO	0.85	0.54	0.55	0.58	0.53	0.47	0.56	0.65
CaO	1.70	1.29	2.61	1.49	1.25	1.20	1.24	2.69
Na_2O	3.80	4.25	4.08	4.34	4.14	4.32	4.31	4.48
K_2O	6.40	6.57	6.44	6.32	6.47	6.13	6.35	5.94
P_2O_5	0.16	0.13	0.13	0.15	0.13	0.15	0.14	0.19
LOI	0.00	0.62	1.85	0.84	0.83	0.57	0.89	0.76
Total	96.69	100.38	100.01	98.38	101.31	98.20	100.24	100.91
V	0.0	37.7	28.9	24.4	21.6	17.1	29.8	46.0
Sc	0.0	6.6	9.6	9.0	9.2	6.4	12.1	7.1
Ba	0.0	913.1	899.8	944.2	941.2	954.4	968.3	1099.8
La	0.0	69.4	65.5	60.0	62.1	62.5	66.6	60.4
Nd	0.0	54.2	0.0	0.0	0.0	0.0	0.0	0.0
Ce	0.0	135.7	130.2	0.0	131.3	0.0	123.9	0.0
Cr	0.0	7.8	12.9	10.3	10.1	34.7	10.4	12.1
Co	0.0	18.6	38.6	12.3	27.9	13.3	17.4	21.5
Ni	0.0	7.6	7.5	7.0	7.7	5.8	8.5	7.5
Cu	0.0	15.2	12.9	16.8	14.7	14.1	17.5	16.7
Zn	0.0	53.2	62.7	58.5	56.3	55.2	51.7	46.5
Ga	0.0	18.4	18.4	20.6	17.9	18.2	17.5	22.9
Pb	0.0	63.7	45.6	66.8	74.9	69.2	52.6	44.0
Th	0.0	36.4	33.8	35.3	36.5	35.0	31.3	47.3
Rb	0.0	243.0	222.4	240.8	228.8	236.5	219.0	254.0
Sr	0.0	228.2	233.3	250.0	220.2	237.6	244.5	650.8
Y	0.0	36.3	39.5	36.4	38.7	35.8	36.0	28.5
Zr	0.0	434.5	369.1	420.8	383.9	418.1	359.7	465.6
Nb	0.0	20.4	19.8	19.3	20.1	18.9	19.7	26.5
Q	11.1	12.3	9.4	10.8	13.9	12.9	12.4	9.9
or	37.8	38.8	38.1	37.3	38.2	36.2	37.5	35.1
ab	32.2	36.0	34.5	36.7	35.0	36.6	36.5	37.9
an	7.4	5.6	7.1	4.3	5.3	5.0	5.2	8.7
C	0.1	0.6	0.0	0.0	1.3	0.1	1.0	0.0
di	0.0	0.0	4.3	1.8	0.0	0.0	0.0	2.9
hy	6.4	5.0	3.9	4.8	5.1	5.2	5.1	3.8
il	1.4	1.3	1.3	1.4	1.3	1.3	1.3	1.4
ap	0.4	0.3	0.3	0.3	0.3	0.3	0.3	0.4

	Osiris Tuff							
Sample	AP64	AP90	AP91v	AP100	AP101v	AP102	AP103	AP110
SiO_2	63.51	63.52	61.58	63.90	64.32	64.86	64.12	63.44
TiO_2	0.75	0.76	0.73	0.72	0.72	0.75	0.72	0.74
Al_2O_3	17.51	17.70	17.53	17.51	16.12	17.17	15.85	17.46
FeO	2.46	2.53	2.42	2.45	2.25	2.73	2.22	2.39
MnO	0.07	0.05	0.05	0.06	0.06	0.06	0.07	0.04
MgO	0.66	0.80	0.93	0.72	0.78	0.59	0.82	0.70
CaO	2.76	2.92	3.25	2.73	1.99	2.33	1.99	3.03
Na_2O	4.24	4.20	3.93	4.26	3.81	4.27	3.60	4.23
K_2O	5.92	5.91	5.48	5.84	5.99	6.06	6.33	5.96
P_2O_5	0.18	0.21	0.15	0.19	0.13	0.16	0.28	0.14
LOI	1.34	0.54	2.72	0.61	3.38	0.75	3.80	1.13
Total	99.40	99.14	98.77	98.99	99.55	99.73	99.80	99.26
V	52.5	52.4	46.0	47.8	39.0	53.2	51.3	38.2
Sc	9.4	7.6	7.7	5.7	6.1	5.4	3.0	5.2
Ba	1095.5	1134.9	1081.8	1205.5	963.0	1088.6	1095.3	1034.3
La	60.6	55.4	52.8	63.9	65.5	62.9	59.5	60.2
Nd	41.1	47.8	0.0	0.0	0.0	0.0	46.2	0.0
Ce	117.7	120.5	0.0	0.0	0.0	0.0	121.5	0.0
Cr	11.3	14.4	7.8	80.4	8.1	130.2	6.1	2.7
Co	18.3	20.8	28.2	22.5	24.1	20.7	18.8	21.0
Ni	8.4	7.5	7.0	9.6	6.0	8.8	8.3	7.3
Cu	17.9	16.9	70.4	15.1	10.1	14.1	15.6	14.8
Zn	42.0	41.8	49.2	40.7	51.3	40.6	42.3	38.6
Ga	20.6	19.1	19.8	20.7	20.4	20.7	20.9	18.9
Pb	49.3	47.1	47.5	72.8	59.7	48.3	50.9	28.4
Th	45.3	45.3	40.7	45.7	56.0	48.8	44.1	44.9
Rb	251.3	248.1	219.7	252.5	279.2	264.9	244.6	236.5
Sr	620.7	665.0	691.0	670.8	374.8	577.4	602.5	566.7
Y	28.9	29.4	26.1	27.0	31.2	30.2	27.5	26.9
Zr	459.6	463.3	415.9	459.7	560.0	498.6	449.4	423.3
Nb	25.8	26.4	24.3	25.8	29.4	27.6	25.6	25.0
Q	8.5	8.3	8.6	9.0	12.8	9.8	12.9	8.1
or	35.0	34.9	32.4	34.5	35.4	35.8	37.4	35.2
ab	35.9	35.5	33.3	36.0	32.2	36.1	30.5	35.8
an	11.3	12.0	14.0	11.4	9.0	9.8	8.0	11.1
C	0.0	0.0	0.0	0.0	0.1	0.0	0.1	0.0
di	1.1	0.9	0.9	0.8	0.0	0.6	0.0	2.6
hy	4.5	5.0	5.2	4.8	5.0	5.0	5.1	3.7
il	1.4	1.4	1.4	1.4	1.4	1.4	1.4	1.4
ap	0.4	0.5	0.3	0.4	0.3	0.4	0.6	0.3

	Osiris	Olivine Basalt						
Sample	AP140v	AP6	AP8	AP9	AP10	AP25	AP26	AP32
SiO_2	63.56	49.14	47.67	51.02	49.96	47.34	48.08	47.27
TiO_2	0.76	1.36	1.57	1.60	1.52	1.23	1.23	1.27
Al_2O_3	16.85	13.94	14.44	16.81	16.47	14.41	14.49	13.65
FeO	2.64	8.48	9.48	9.11	9.12	8.12	8.21	8.46
MnO	0.06	0.15	0.17	0.16	0.17	0.14	0.15	0.15
MgO	0.99	9.74	9.63	3.97	4.89	10.01	9.96	10.09
CaO	2.64	8.68	8.73	7.49	8.59	10.88	9.99	10.35
Na_2O	4.52	2.89	3.21	4.07	3.48	2.91	2.96	2.98
K_2O	4.99	2.03	1.34	2.32	2.21	1.88	1.97	1.88
P_2O_5	0.14	0.53	0.57	0.90	0.56	0.62	0.66	0.63
LOI	3.38	1.18	1.87	1.47	1.90	2.02	1.26	1.70
Total	100.53	98.12	98.68	98.92	98.87	99.56	98.96	98.43
V	41.8	205.5	200.8	206.9	258.3	222.7	216.1	202.6
Sc	4.4	19.8	21.5	17.2	20.2	22.0	28.2	21.1
Ba	1019.5	1287.2	1253.4	1951.7	1726.0	1407.0	1544.2	1276.8
La	51.2	61.6	46.2	82.0	50.0	68.0	80.4	62.2
Ce	0.0	0.0	0.0	0.0	0.0	0.0	153.6	0.0
Cr	19.2	379.1	387.9	22.6	88.0	544.4	513.3	400.2
Co	18.5	52.8	51.1	35.2	49.6	52.4	62.0	50.1
Ni	8.6	234.6	225.6	18.2	45.8	214.5	237.0	261.3
Cu	17.3	54.6	52.3	28.8	50.0	51.4	55.6	47.5
Zn	89.8	80.2	84.6	103.8	86.1	84.0	86.4	79.1
Ga	18.8	16.3	17.4	24.2	20.8	16.7	16.5	18.7
Pb	56.6	13.4	6.4	16.7	11.4	13.5	11.9	9.2
Th	50.6	9.4	8.2	11.1	6.8	4.2	7.2	6.3
Rb	259.3	56.1	19.1	36.3	46.0	42.4	42.7	41.0
Sr	518.7	780.6	838.2	1352.0	967.6	1330.1	1535.3	1261.4
Y	29.5	23.3	23.4	26.6	23.8	24.5	22.6	24.4
Zr	501.4	147.3	170.7	175.2	147.2	136.2	144.0	126.2
Nb	27.5	30.6	31.2	29.6	24.6	16.9	16.5	18.3
Q	10.0	0.0	0.0	0.0	0.0	0.0	0.0	0.0
or	29.5	12.0	7.9	13.7	13.1	11.1	11.6	11.1
ab	38.3	23.0	23.1	34.1	27.7	12.3	16.3	13.9
an	10.9	19.1	21.0	20.8	22.8	20.7	20.4	18.3
ne	0.0	0.8	2.2	0.2	0.9	6.7	4.7	6.1
di	1.0	16.7	15.1	8.8	13.4	23.7	20.1	23.5
hy	5.7	0.0	0.0	0.0	0.0	0.0	0.0	0.0
ol	0.0	21.6	23.1	14.8	14.8	19.3	20.6	19.9
il	1.4	2.6	3.0	3.0	2.9	2.3	2.3	2.4
ap	0.3	1.2	1.3	2.1	1.3	1.4	1.5	1.5

	Olivine Basalt							
Sample	AP45	AP52	AP54	AP55	AP58	AP76	AP78	AP80
SiO_2	47.56	46.31	54.49	49.55	48.58	46.14	45.16	46.80
TiO_2	1.46	1.57	1.15	1.30	1.40	1.53	1.48	1.31
Al_2O_3	15.36	14.20	14.89	15.57	14.31	15.09	13.74	14.36
FeO	9.07	9.30	6.99	8.02	9.75	9.33	8.88	8.55
MnO	0.17	0.17	0.13	0.14	0.17	0.16	0.17	0.16
MgO	10.28	10.05	5.72	6.06	8.99	9.62	9.59	9.95
CaO	10.38	9.97	8.16	10.76	9.13	9.21	12.17	9.47
Na_2O	2.55	3.51	3.57	3.52	2.84	2.81	3.06	2.68
K_2O	1.66	0.87	2.36	2.25	1.95	1.88	1.00	2.32
P_2O_5	0.67	0.60	0.55	0.67	0.63	0.49	0.84	0.63
LOI	1.69	2.28	0.28	1.79	0.43	1.77	2.10	2.05
Total	100.85	98.83	98.29	99.63	98.18	98.03	98.19	98.28
V	225.4	226.1	162.0	191.9	186.2	215.7	244.8	208.7
Sc	29.8	25.3	2.8	22.7	25.0	26.9	30.1	26.2
Ba	1506.6	1387.5	1550.7	1979.2	1301.8	1443.2	2292.0	1922.2
La	50.9	48.0	63.1	86.7	58.6	39.4	95.0	61.1
Cr	427.9	404.7	168.0	238.4	343.9	281.0	379.9	362.3
Co	59.1	49.3	56.4	41.4	49.0	52.5	52.6	48.3
Ni	212.0	213.2	68.0	63.4	180.5	183.2	170.5	203.3
Cu	47.3	45.1	45.4	35.2	44.1	46.6	43.3	49.5
Zn	80.4	70.8	75.3	81.8	92.1	73.7	72.8	71.1
Ga	17.4	15.8	20.1	18.2	19.0	17.2	15.9	17.7
Pb	6.0	14.3	15.4	15.4	9.1	5.0	9.3	9.1
Th	3.9	6.8	11.7	12.4	6.2	9.3	10.7	10.3
Rb	41.7	41.1	53.0	42.8	49.9	61.0	20.8	58.6
Sr	928.0	945.6	1075.5	1659.7	1064.9	868.3	1640.4	1222.8
Y	28.7	25.7	20.1	24.8	23.2	27.5	25.0	22.4
Zr	182.5	172.3	119.0	114.9	141.6	162.0	124.2	163.8
Nb	31.0	32.6	23.4	22.0	24.0	32.9	35.3	27.6
or	9.8	5.1	13.9	13.3	11.5	11.1	5.9	13.7
ab	15.8	18.2	30.2	18.8	21.2	14.6	10.9	13.3
an	25.6	20.4	17.6	20.0	20.5	23.0	20.8	20.3
ne	3.1	6.2	0.0	5.9	1.5	5.0	8.1	5.1
di	17.5	20.4	15.8	23.8	16.9	15.9	27.7	18.3
hy	0.0	0.0	15.0	0.0	0.0	0.0	0.0	0.0
ol	23.0	21.7	1.9	11.9	21.9	22.7	17.9	21.6
il	2.8	3.0	2.2	2.5	2.7	2.9	2.8	2.5
ap	1.5	1.4	1.3	1.5	1.5	1.1	2.0	1.5

	Olivine Basalt							
Sample	AP107	AP127	AP131	AP133	AP142	AP143	A1	A2
SiO_2	49.12	46.68	48.43	47.04	53.88	51.71	49.26	48.13
TiO_2	1.33	1.49	1.27	1.55	1.43	1.44	1.39	1.29
Al_2O_3	16.58	16.15	15.97	14.73	17.05	16.62	16.18	15.96
FeO	10.23	9.10	10.11	9.11	8.27	8.22	9.07	8.11
MnO	0.18	0.17	0.17	0.17	0.14	0.15	0.16	0.15
MgO	7.92	9.09	8.76	10.54	3.86	4.02	8.13	8.46
CaO	9.93	9.64	9.61	10.19	7.25	7.52	9.77	8.56
Na_2O	3.16	3.14	2.76	2.69	4.26	4.20	3.15	3.06
K_2O	1.39	2.52	1.40	1.75	2.43	2.57	1.95	2.63
P_2O_5	0.45	0.49	0.46	0.65	0.82	0.82	0.52	0.59
LOI	0.76	1.87	0.01	1.00	1.46	1.14	0.95	1.42
Total	101.05	100.34	98.95	99.42	100.85	98.41	100.53	98.36
V	207.7	207.9	177.3	252.3	202.5	169.1	207.6	170.5
Sc	26.6	23.5	27.8	24.8	17.9	16.8	23.3	21.4
Ba	1133.8	2360.1	1127.6	1467.6	1971.9	1855.0	1569.5	2187.8
La	46.5	72.8	39.6	68.8	91.7	83.6	51.1	49.9
Nd	0.0	59.8	0.0	0.0	0.0	0.0	0.0	0.0
Ce	0.0	144.0	0.0	0.0	0.0	0.0	0.0	0.0
Cr	260.0	270.9	354.7	452.4	31.2	29.2	262.8	257.8
Co	53.5	51.8	50.2	59.8	30.0	31.8	50.3	36.5
Ni	136.3	146.3	158.3	231.3	24.6	25.8	138.6	146.7
Cu	55.9	49.2	67.2	50.9	33.0	30.4	41.9	39.7
Zn	86.6	71.1	80.0	87.0	108.2	96.0	77.2	65.2
Ga	21.4	14.9	20.4	19.0	21.4	21.6	15.5	17.8
Pb	6.6	8.1	7.2	13.8	22.6	18.1	16.3	8.8
Th	5.1	8.3	5.2	7.2	13.6	11.3	5.6	7.8
Rb	31.5	95.5	31.1	43.3	53.4	53.4	43.3	73.6
Sr	881.9	1357.1	891.8	1041.9	1309.7	1272.5	890.0	900.1
Y	27.2	31.0	26.2	28.8	26.3	27.1	26.2	26.2
Zr	129.5	208.8	125.5	173.5	186.2	179.3	238.3	197.5
Nb	19.9	42.2	19.2	32.8	30.4	29.2	26.8	40.0
or	8.2	14.9	8.3	10.3	14.4	15.2	11.5	15.5
ab	21.8	6.4	21.8	14.2	36.0	33.6	17.4	17.4
an	27.0	22.5	27.0	23.0	20.2	18.9	24.3	22.0
ne	2.7	10.9	0.9	4.7	0.0	1.1	5.0	4.6
kal	0.0	0.0	0.0	0.0	0.0	0.0	19.8	13.5
di	15.9	20.6	14.4	19.0	13.2	10.9	0.0	0.0
hy	0.0	0.0	0.0	0.0	0.4	0.0	18.4	20.0
ol	21.1	19.8	23.1	22.9	11.6	13.0	0.0	0.0
ac	0.0	0.0	0.0	0.0	0.0	0.0	2.6	2.5
il	2.5	2.8	2.4	2.9	2.7	2.7	0.0	0.0
hem	0.0	0.0	0.0	0.0	0.0	0.0	0.0	1.4
ap	1.0	0.0	1.1	1.5	0.0	1.9	0.0	0.0

	Olivine Basalt				
Sample	A3	A4	A5	A6	A7
SiO_2	49.17	48.97	48.63	47.34	48.80
TiO_2	1.43	1.43	1.39	1.37	1.38
Al_2O_3	16.10	15.80	15.64	15.44	15.76
FeO	9.36	9.34	8.98	8.99	9.32
MnO	0.16	0.16	0.17	0.16	0.17
MgO	8.61	9.17	8.29	8.57	8.53
CaO	9.33	9.30	9.76	8.81	9.69
Na_2O	3.20	3.23	3.31	2.96	2.74
K_2O	1.90	1.65	1.23	1.83	1.86
P_2O_5	0.52	0.57	0.56	0.54	0.53
LOI	0.44	0.61	1.64	0.33	2.40
Total	100.22	100.23	99.60	96.34	101.18
V	211.3	191.2	187.6	177.4	162.4
Sc	25.9	23.7	26.4	22.5	21.1
Ba	1567.7	1617.1	1573.7	1512.8	1331.5
La	43.8	51.8	50.2	50.7	42.6
Cr	271.4	285.0	290.2	259.0	296.1
Co	49.8	51.1	48.0	50.9	40.6
Ni	151.3	178.3	174.1	154.5	162.1
Cu	40.8	43.5	43.2	46.9	49.2
Zn	79.0	71.7	70.9	67.2	72.6
Ga	17.2	16.7	17.2	17.7	15.8
Pb	21.8	16.5	20.8	16.3	6.4
Th	2.7	3.3	3.2	3.8	5.6
Rb	40.4	30.5	19.2	40.6	38.6
Sr	903.0	1001.0	947.6	862.1	920.9
Y	26.3	25.8	25.0	25.6	27.8
Zr	228.2	250.4	247.2	220.2	159.8
Nb	26.5	27.2	27.3	25.4	26.6
or	11.2	9.8	7.3	10.8	11.0
ab	18.0	18.8	21.2	17.9	20.5
an	24.0	23.7	24.2	23.4	25.2
ne	4.9	4.6	3.7	3.9	1.5
kal	18.3	18.3	19.8	16.6	15.9
hy	20.2	21.1	18.6	20.3	20.9
ac	2.7	2.7	2.6	2.6	2.6
hem	0.0	0.0	0.0	0.0	1.2

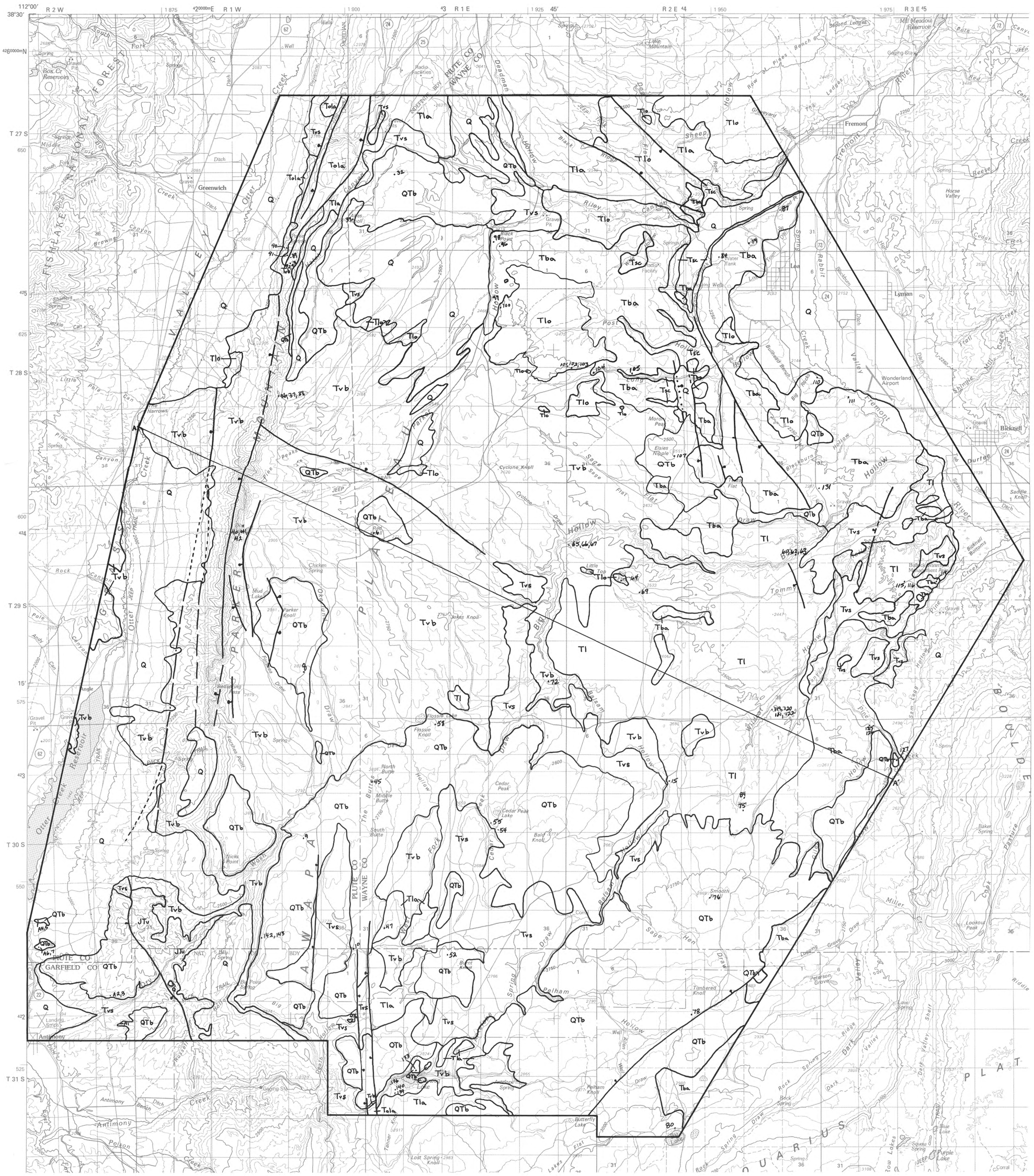

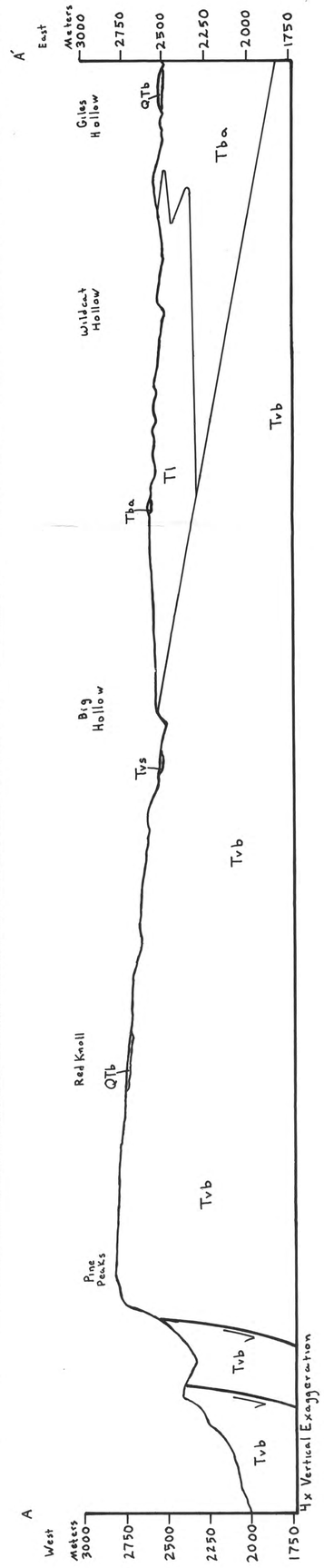

DESCRIPTION OF MAP UNITS

JTu = Jurassic - Triassic undifferentiated
Tsc = Sandstone, siltstone, conglomerate
Tvb = Andesite breccia = volcanic rocks of Langdon Mountain, alluvial facies
Tba = Basaltic andesite
Tola = Osiris Tuff, latite, and basaltic andesite flows undifferentiated
Tla = Latite and basaltic andesite flows undifferentiated
Tl = Latite
Tlo = Osiris Tuff
Tvs = Volcanic sediment = Sevier River Formation
QTb = Olivine basalt
Q = Quaternary deposits undifferentiated

Plate 1. LOCATION OF AWAPA PLATEAU SAMPLES

SCALE 1:100,000

KILOMETERS

MILES

Utah Geological Survey
Miscellaneous Publication 91-5, 1991

Base map from U.S. Geological Survey, Loa 1:100,000
Geology from Williams and Hackman, 1971, SCALE 1:250,000